The Radiopharmaceutical Chemistry of Technetium-99m

Stephanie M. Rathmann, Zainab Ahmad, Samantha Slikboer, Holly A. Bilton, Denis P. Snider, and John F. Valliant

Nuclear Chemistry

Isotopes of Technetium

Technetium, a transition metal, is the 43rd element in the periodic table and was the first synthetic element reported [1]. It has a $4d^5 5s^2$ (d^7) electron configuration and forms a wide variety of coordination and organometallic complexes [2–4]. Remarkably, there are 51 isotopes of technetium ranging from technetium-85 to technetium-120. Of these, the two most studied are technetium-99—which has a half-life of 211,000 y and is sometimes referred to as technetium-99g—and ^{99m}Tc. The latter is our primary concern here. The half-life of ^{99m}Tc is 6.01 h and is nearly ideal for nuclear medicine. Indeed, it is long enough to facilitate the preparation, transportation, and administration of radiopharmaceuticals as well as the imaging of patients. At the same time, it is short enough to allay concerns surrounding radiation exposure and disposal. In addition, the primary gamma rays emitted by ^{99m}Tc have an energy of 140 keV, which is sufficient to allow for clinical tomographic whole-body imaging at any depth without imparting a burdensome radiation dose. These features—along with its low cost and widespread availability—have made ^{99m}Tc one of the most important radionuclides in clinical diagnostic nuclear medicine [5]. Across the globe, approximately 25 million medical imaging procedures are performed using ^{99m}Tc-based radiopharmaceuticals every year [5, 6].

S. M. Rathmann · Z. Ahmad · S. Slikboer · H. A. Bilton
D. P. Snider · J. F. Valliant (✉)
Department of Chemistry and Chemical Biology, McMaster University, Hamilton, ON, Canada
e-mail: valliant@mcmaster.ca

Method of Production

It is critical that any radionuclide destined for routine clinical use have a plentiful and secure supply at reasonable cost. ^{99m}Tc is a daughter radionuclide formed via the β^--emission of molybdenum-99 (^{99}Mo) [7]. There are two principal ways in which ^{99}Mo is produced: (i) as a by-product of nuclear fission or (ii) via the direct irradiation of molybdenum-98 in a nuclear reactor. In the former case, ^{99}Mo can be isolated from the fission of uranium-235 in a nuclear reactor with a yield of 6% [8]. In the latter case, molybdenum-98 is bombarded with neutrons to produce ^{99}Mo. This method requires intense neutron sources to generate sufficient amounts of ^{99}Mo [9]. The recent global shortage of ^{99}Mo has spurred the development of alternative strategies for the production of ^{99}Mo, including production using linear accelerators [10]. Here, a molybdenum-100 (^{100}Mo) source is irradiated with gamma rays, resulting in the release of a neutron in what is otherwise known as the ^{100}Mo(γ,n)^{99}Mo reaction. The direct production of ^{99m}Tc on cyclotrons is also a possibility. In this scenario, the proton bombardment of a solid ^{100}Mo source—the ^{100}Mo(p,2n)^{99m}Tc reaction—is used [8, 11].

The ^{99}Mo/^{99m}Tc Generator

The ^{99}Mo/^{99m}Tc generator is a convenient way to obtain ^{99m}Tc and is one key reason that ^{99m}Tc became one of the most widely used in nuclear imaging. A ^{99}Mo/^{99m}Tc generator contains ^{99}Mo—in the form of molybdate $[^{99}Mo]MoO_4^{2-}$—absorbed onto an aluminum oxide column. Importantly, the product formed via the decay of the ^{99}Mo is $[^{99m}Tc]TcO_4^-$ that does not have the same affinity for the aluminum oxide. As a result, the $[^{99m}Tc]TcO_4^-$ can be eluted from the generator in high purity [12]. Conveniently, a simple 0.9% saline (9 mg/ml NaCl) solution can be used to selectively elute the $[^{99m}Tc]TcO_4^-$. A schematic of a ^{99}Mo/^{99m}Tc generator and series of photographs depicting how it is used are shown in Fig. 1 (see the section on "Eluting a ^{99}Mo/^{99m}Tc Generator"

J. S. Lewis et al. (eds.), *Radiopharmaceutical Chemistry*, https://doi.org/10.1007/978-3-319-98947-1_18

for more details). ^{99}Mo/^{99m}Tc generators are typically eluted once every 24 h, but it is possible to do 2–3 elutions per day. Depending on the "size" of the generator (*i.e.* the activity of ^{99}Mo), sufficient ^{99m}Tc can be obtained to produce 50–80 patient doses per day.

The Chemistry of Technetium

General

Technetium complexes have been reported with oxidation states ranging from −1 to +7 [13]. Examples highlighting the diversity of ^{99m}Tc chemistry are shown in Table 1. The oxidation state formed when working with ^{99m}Tc—as is the case for other transition metals—is controlled by several factors, including pH, the type and "strength" of the reducing agent, and the nature of the coordinating ligands [14]. The structures of technetium complexes vary widely. Indeed, ^{99m}Tc complexes with tetrahedral (N = 4), tetragonal pyramidal (N = 5), octahedral (N = 6), capped octahedral (N = 7), and pentagonal bipyramidal (N = 8) geometries have been reported [15]. The formation of multiple structural isomers is also common, which must be taken into account when designing ^{99m}Tc-based radiopharmaceuticals. For example, for Tc(V) complexes of amino acid-based chelators—such as [^{99m}Tc]TcO(RP294)—it is possible to form both *syn*- and *anti*-isomers (Fig. 2) [16]. Such isomers can create substantial issues (particularly at the stage of regulatory approval), as they may have different physical and biochemical properties.

Characterizing ^{99m}Tc Complexes

Characterizing ^{99m}Tc complexes can be a challenge because the doses used for nuclear imaging typically contain only a very small molar amount of the metal complex. For instance, the dose of a ^{99m}Tc-labeled radiopharmaceutical used for a clinical scan—typically, 185–925 MBq—corresponds to only 0.95–4.7 nanograms (ng) of metal. This is below the detection limit of methods typically used for the macroscopic characterization of metal complexes. Furthermore, as there are no stable isotopes of technetium, ^{99}Tc must be used to develop new complexes and study the chemistry of ^{99m}Tc. ^{99}Tc has a half-life of 2.11×10^5 years, and because it undergoes a low-energy beta decay, it can be easily shielded, and milligram quantities can be handled safely. However, the long half-life does create challenges with regard to contamination and disposal. Consequently, rhenium, technetium's 5d congener, is often used to prepare reference standards for ^{99m}Tc-containing compounds.

Re and Tc have similar atomic radii due to the lanthanide contraction and regularly form structurally analogous complexes. A notable exception to the similarity in their chemistry

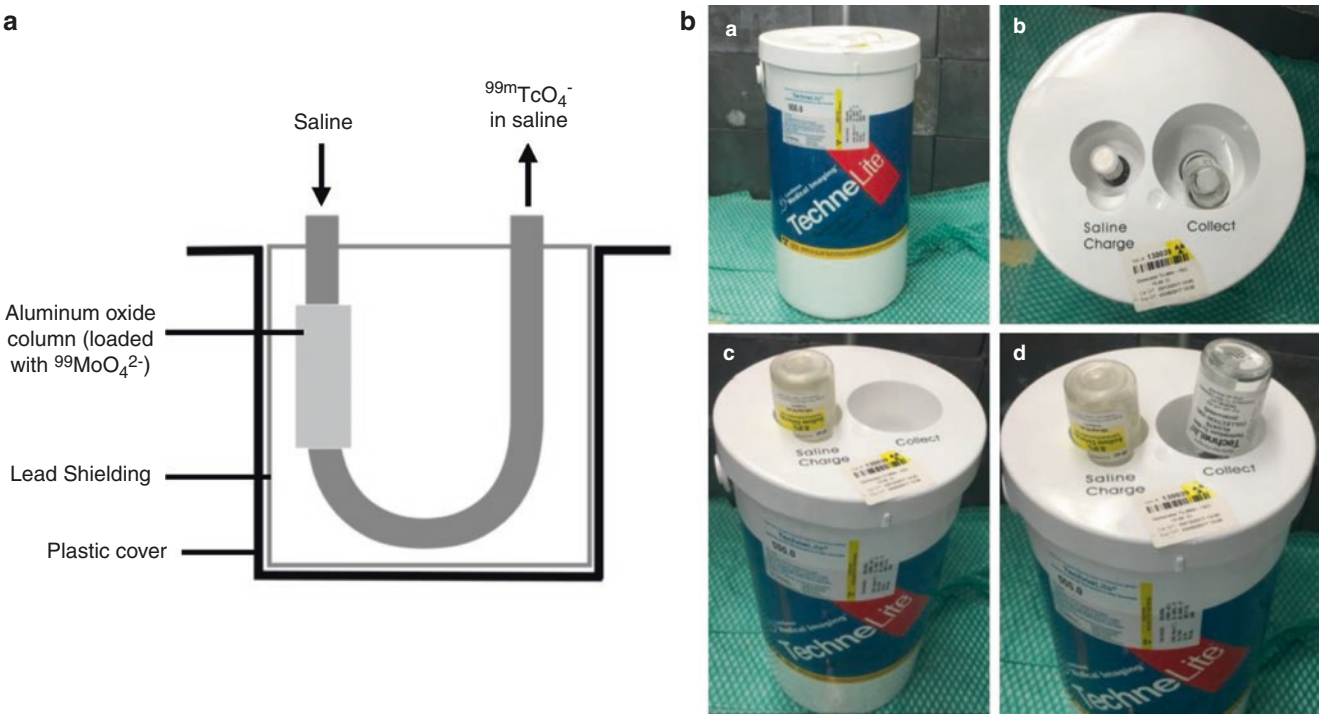

Fig. 1 ^{99}Mo/^{99m}Tc generator. (**a**) Schematic representation of a ^{99}Mo/^{99m}Tc generator. (**b**). A typical ^{99}Mo/^{99m}Tc generator. (**a**) Side view; (**b**) top view; (**c**) vial of saline containing the desired volume to elute attached to the inlet; (**d**) ^{99m}Tc collection vial attached to collection port (Note that the collection vial is often enclosed in a specially designed lead pig)

is the fact that ReO_4^- is harder to reduce than TcO_4^-. This can require the use of different reducing agents and reaction conditions to prepare analogous Re and Tc complexes. For example, the preparation of the ^{99m}Tc(I)- and Re(I)-based analogues of $[(M(CO)_3(OH_2)_3]^+$ requires significantly different conditions and reagents [17–19]. For the ^{99m}Tc complex, the product can be prepared in a single step using boranocarbonate ($[CO_2BH_3]^{2-}$). For radioisotopes of Re, however, a two-step kit must be used since it is necessary to first employ a mixture H_3PO_4 and BH_3-NH_3 to get the second step (treatment with boranocarbonate) to proceed in high yield [14, 20]. Re(V) and Tc(V) chelator complexes are similarly prepared under different conditions, as the formation of complexes of Re(V) often requires higher temperatures, lower pH, and higher concentrations of reducing agents than complexes of Tc(V) [19]. Another important difference between the chemistries of Tc and Re is that it is common for analogous complexes of each element to have disparate stabilities toward oxidation and disproportionation reactions [21].

When developing a new ^{99m}Tc-based radiopharmaceutical, convention dictates that a Re analogue be prepared on a multi-milligram scale and characterized by NMR, mass spectrometry, and X-ray crystallography (when possible). Once the ^{99m}Tc-labeled compound is synthesized, both the ^{99m}Tc and Re complexes can be co-injected into an HPLC. Subsequently, the elution of the Re complex can be monitored via UV or MS, the elution of the ^{99m}Tc complex can be monitored using a radiation detector, and their retention times can be compared to verify co-elution.

Table 1 The oxidation states of technetium and examples of different Tc complexes

Oxidation state	Archetypal examples	Application in nuclear medicine
−1	$[Tc(CO)_5]^-$	N/A
0	$Tc_2(CO)_{10}$	N/A
+1	$[Tc(CO)_3(H_2O)_3]^+$, $[Tc(CNCH_2C(CH_3)_2OCH_3)_6]^+$	Prostate cancer, cardiac imaging
+2	$[TcCl_4]^{2-}$, $[Bu_4N][Tc(NO)Br_4]$	N/A
+3	Teboroxime, $[TcCl_3(Et_2PhP)_3]$	Myocardial perfusion
+4	Bisphosphonates,$[TcO(OH)EDTA]^{3-}$	Bone injury and metabolism
+5	Tc-MAG_3, Tc-BAT	Renal function, brain imaging
+6	TcF_6, $[TcNCl_4]^-$	N/A
+7	TcO_4^-	Thyroid imaging

N/A = Not applicable

Current ^{99m}Tc-Based Radiopharmaceuticals: Structure, Synthesis, and Clinical Use

^{99m}Tc-based radiopharmaceuticals have dominated the field of nuclear medicine for the past several decades, though recent advances in the use of radionuclides for positron emission tomography (PET) have changed this predominant role [5, 22]. Notwithstanding, ^{99m}Tc-labeled agents are used daily around the globe to diagnose a wide spectrum of pathologies, including ischemia, coronary artery disease, renal failure, bone disease and fractures, cerebrovascular diseases, liver and gall bladder disorders, and cancer.

^{99m}Tc-based radiopharmaceuticals are obtained using "instant kits," which facilitate robust and high-yielding ^{99m}Tc-labeling reactions using simple and typically one-step procedures [23]. This technology—as with ^{99}Mo/^{99m}Tc generators—greatly simplified the production and ease of access to ^{99m}Tc-based radiopharmaceuticals. These kits typically contain a lyophilized mixture of the compound (ligand) to be labeled, buffers, and various additives. The latter include antioxidants (to increase stability of the product), catalysts, solubilizing agents, and fillers (for quick solubilization prior to lyophilization when preparing the kits). The buffers utilized in these kits are crucial, as the pH of the reaction mixture following the addition of the metal can have a significant influence on the yield of the radiolabeling reaction, as well as how simple and multifunctional ligands coordinate ^{99m}Tc. Detailed information regarding specific additives for approved radiopharmaceuticals can be found in the package inserts, which are referenced for the examples provided below.

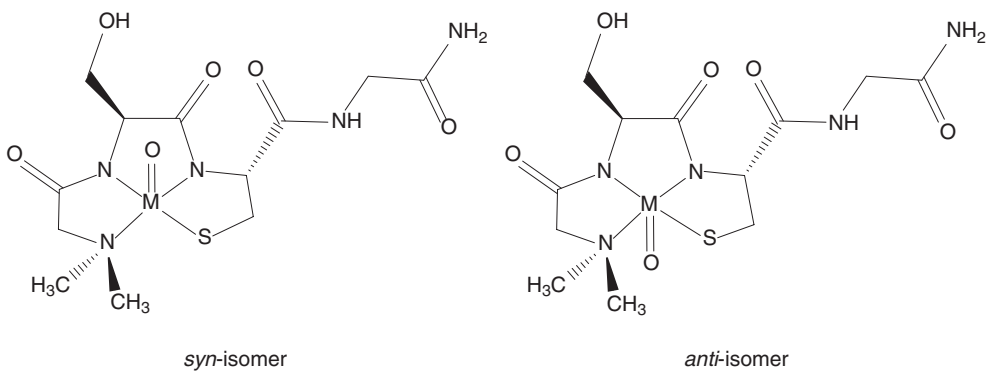

Fig. 2 The *syn*- and *anti*-isomers of [^{99m}Tc]TcO(RP294)

Agents for Cardiac Perfusion Imaging

[^{99m}Tc]Tc-Sestamibi

[^{99m}Tc]Tc-Sestamibi (Cardiolite™) is an approved radiopharmaceutical used primarily for the imaging of myocardial perfusion. In this context, it can be used to identify both cardiac ischemia and necrosis by comparing SPECT images collected during resting and stress (postexercise) states. Interestingly, it is also often employed as a second-line diagnostic for the imaging of breast tumors after positive mammography [24]. [^{99m}Tc]Tc-Sestamibi is an octahedral, cationic ^{99m}Tc(I) complex (Fig. 3a) that was developed as a replacement for an older cardiac imaging agent—[^{201}Tl]TlCl (thallous chloride)—because it produces images of superior quality and reduces radiation doses to patients [25, 26]. [^{99m}Tc]Tc-Sestamibi accumulates in tissues in proportion to blood flow by localizing quickly within the mitochondria of cardiomyocytes [24, 27]. In healthy patients, it clears primarily through both the hepatobiliary (33%) and renal (27%) systems with a blood half-life of 4.3 min at rest and 1.6 min following exercise-induced stress [27].

[^{99m}Tc]Tc-Sestamibi contains six isonitrile ligands and is a unique example of an organometallic complex that can be prepared in water under dilute conditions. It is produced using a high-yielding, single-step instant kit, which contains the isonitrile ligands as their copper(I) complex, a series of buffers and antioxidants, and stannous chloride as the reducing agent. [^{99m}Tc]TcO_4^- in saline is added to the kit to form the product, and the purity of the final radiopharmaceutical is verified by instant thin layer chromatography (iTLC) [27]. iTLC, which typically employs silica-impregnated chromatography paper, is a rapid and convenient method for determining the purity of radiopharmaceuticals [23].

[^{99m}Tc]Tc-Tetrofosmin

[^{99m}Tc]Tc-Tetrofosmin (Myoview™), like [^{99m}Tc]Tc-sestamibi, is an approved agent used for myocardial perfusion imaging. Specifically, it is used to identify regions of reversible myocardial ischemia and infarcted myocardium in patients with suspected coronary artery disease [28, 29] In addition, it is used for evaluating ventricular function in patients with known or suspected heart disease [30]. As shown in Fig. 3b, [^{99m}Tc]Tc-tetrofosmin—([^{99m}Tc]Tc-(tetrofosmin)$_2O_2$)$^+$—is a cationic, trans-dioxo-bis(diphosphine)-technetium(V) complex [28–30]. It is prepared using a high-yielding kit by combining an ether-functionalized diphosphine ligand (1,2-bis[bis(2-ethoxyethyl)phosphino] ethane) with stannous chloride as the reducing agent, disulfosalicylate as an antimicrobial, and the appropriate buffers. The uptake of [^{99m}Tc]Tc-tetrofosmin is proportional to the blood flow, and its mechanism of uptake and retention is seemingly identical to that of [^{99m}Tc]Tc-sestamibi. Quantitative SPECT imaging with [^{99m}Tc]Tc-tetrofosmin is used to assess the presence of ischemia or necrosis by detecting differing levels of signal in the heart before, during, or after exercise. This radiopharmaceutical shows rapid uptake in the myocardium, quick clearance from the blood, liver, and lungs, and primarily renal excretion.

Agent for Bone Imaging

[^{99m}Tc]Tc-MDP

[^{99m}Tc]Tc-Medronate (DraxImage® MDP-25 and TechneScan® MDP) is a radiopharmaceutical used for bone scintigraphy in which the radiometal is chelated by methylene diphosphonate (Fig. 4) [31]. [^{99m}Tc]Tc-MDP is believed to be a Tc(IV) complex with one ^{99m}Tc atom complexed by two diphosphonate ligands. However, at the macroscopic scale with ^{99}Tc, X-ray crystallography reveals that each diphosphonate ligand is bound to two Tc centers, resulting in a mixture of polymers and oligomers. Importantly, this is not likely to be the structure for [^{99m}Tc]

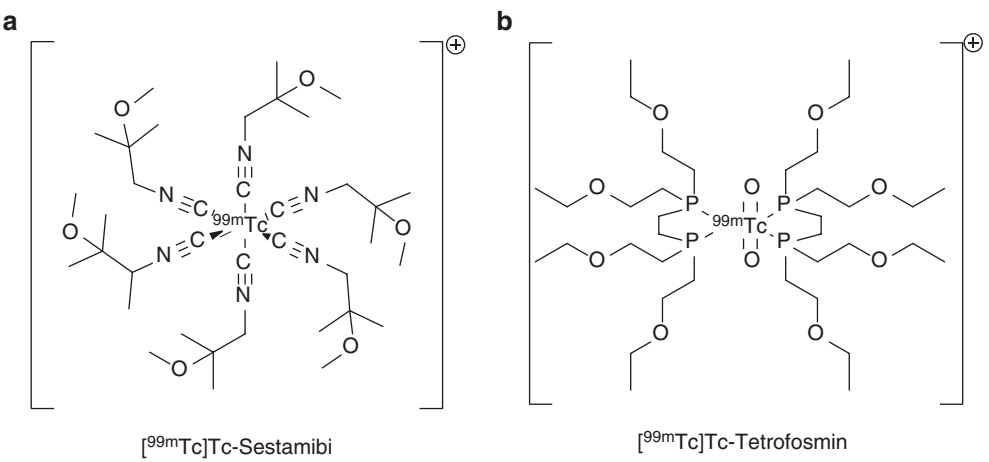

Fig. 3 ^{99m}Tc-labeled cardiac perfusion agents currently used in nuclear medicine. (**a**) [^{99m}Tc]Tc-Sestamibi and (**b**) [^{99m}Tc]Tc-tetrofosmin

Tc-MDP, since the ^{99m}Tc-radiosynthesis reactions are performed using small amounts of the radiometal in the presence of a large excess of ligand [23, 32, 33]. [^{99m}Tc]Tc-MDP is obtained by combining [^{99m}Tc]TcO_4^- with a lyophilized and sterile mixture of medronic acid, ascorbic acid, and stannous fluoride [34]. [^{99m}Tc]Tc-MDP is used to detect bone metastases as well as osteonecrosis because it localizes to the sites of high calcium metabolism, typically by binding to hydroxyapatite [31, 34]. This allows for the imaging of skeletal tumors as well as soft tissue malignant sarcomas and adenocarcinomas in which calcium deposits accumulate. Note that ^{99m}Tc-labeled bisphosphonates can also be used for the imaging of osteomyelitis (infection in the bone) and have recently been reported to accumulate in tumor-associated macrophages found in non-osseous lesions [35].

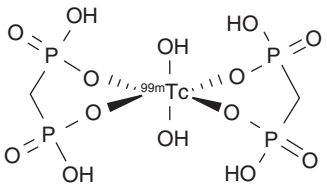

[^{99m}Tc]Tc-MDP

Fig. 4 The ^{99m}Tc-labeled bone scanning agent, [^{99m}Tc]Tc-MDP [23]

Agents for Renal Imaging

[^{99m}Tc]Tc-DMSA

[^{99m}Tc]Tc-DMSA (dimercaptosuccinic acid) is an approved radiopharmaceutical for renal cortical scintigraphy and is largely used for the delineation of renal scars [36, 37]. This radiopharmaceutical is obtained in a kit formulation as a vial containing a lyophilized, sterile mixture of dimercaptosuccinic acid (90% meso-isomer and 10% D- and L-isomers), stannous chloride dihydrate, ascorbic acid, and inositol to which a solution of [^{99m}Tc]TcO_4^- in saline is added. The mixture is incubated for 10 min to obtain the final product (Fig. 5a) [23, 34, 36]. The mechanism of [^{99m}Tc]Tc-DMSA is predicated on the ability of the complex to bind plasma proteins. Once protein-bound, the [^{99m}Tc]Tc-DMSA clears from the plasma and eventually concentrates in the renal cortex by 1 h postinjection, with approximately 20% of injected dose still present in each kidney 6 h following the administration of the radiotracer [36, 38]. [^{99m}Tc]Tc-DMSA is also used to

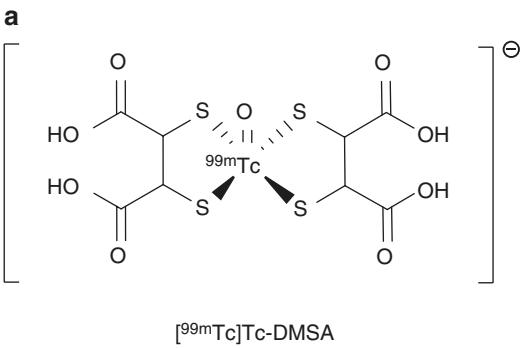

[^{99m}Tc]Tc-DMSA

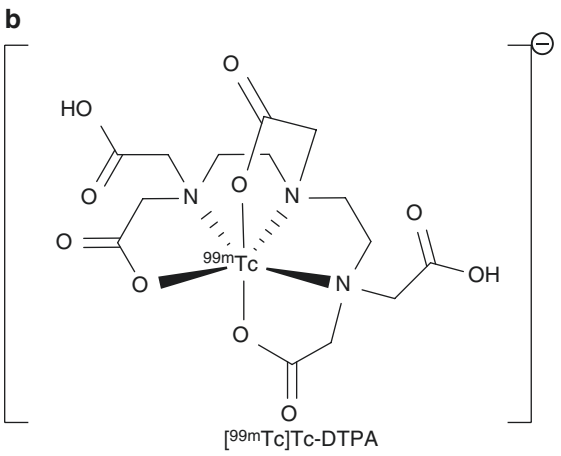

[^{99m}Tc]Tc-DTPA

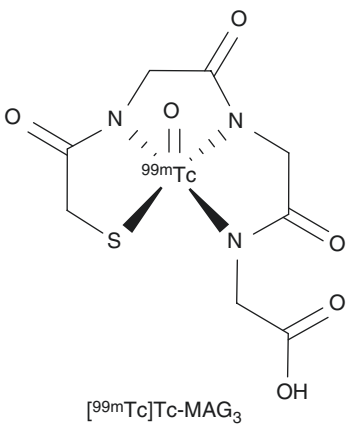

[^{99m}Tc]Tc-MAG_3

Fig. 5 Three ^{99m}Tc-labeled agents used in renal function testing:
(**a**) [^{99m}Tc]Tc-DMSA,
(**b**) [^{99m}Tc]Tc-DTPA, and
(**c**) [^{99m}Tc]Tc-MAG_3

evaluate kidney function, as patients with advanced renal failure will exhibit little renal uptake of the agent [36].

[^{99m}Tc]Tc-DTPA

[^{99m}Tc]Tc-DTPA (diethylenetriaminepentaacetate)—also known as [^{99m}Tc]Tc-Pentetate™—is also an approved radiopharmaceutical used for renal scintigraphy [34, 39, 40]. The product is obtained by adding [^{99m}Tc]TcO_4^- to vials containing diethylenetriaminepentaacetic acid (pentetic acid) as well as buffers, stabilizers, and stannous chloride dehydrate [34, 39, 40]. [^{99m}Tc]Tc-DTPA (Fig. 5b) is administered intravenously and used to assess renal perfusion and glomerular filtration rate. It also has applications for brain imaging, in which it is used to detect intracranial lesions associated with excessive neovascularity or a compromised blood-brain barrier (BBB) [39]. For renal studies, imaging is done within a few minutes of injection because the rapid excretion through the kidneys allows for the assessment of the glomerular filtration rate as well as renal blood flow.

[^{99m}Tc]Tc-MAG_3

[^{99m}Tc]Tc-MAG_3 (^{99m}Tc-mercaptoacetyltriglycine) is a radiopharmaceutical sold under the name of TechneScan MAG_3™ that is also utilized to assess kidney function, notably renal failure and urinary tract obstruction [40–42]. [^{99m}Tc]Tc-MAG_3 renograms are often performed on kidney donors prior to kidney transplantation to evaluate the health of a donor kidney. It is obtained in a kit for formulation with each vial containing a lyophilized and sterile mixture of the ligand, reducing agent, and buffers to maintain a pH between 5 and 6 during labeling [34, 41]. [^{99m}Tc]Tc-MAG_3 is a tetradentate, monooxo complex of Tc(V), and mercaptoacetyltriglycine (Fig. 5c). Like [^{99m}Tc]Tc-DMSA, the mechanism of [^{99m}Tc]Tc-MAG_3 is predicated on the ability of the complex to bind plasma proteins [41, 43]. This binding is reversible, and the unbound complex is cleared quickly from the blood. Healthy individuals have a faster clearance rate in comparison with patients with impaired renal function. Unlike [^{99m}Tc]Tc-DMSA, which stays as a protein-bound complex for imaging purposes, the reversible protein binding and clearing of [^{99m}Tc]Tc-MAG3 from the blood are utilized for assessment of renal function. Thus, the presence of the free hydrophilic metal complex in the blood and subsequent glomerular filtration through the kidneys with active tubular secretion provides data on kidney function and areas of obstruction [41, 44]. The clearance of the compound is correlated with effective renal plasma flow, with 40–50% of the injected dose extracted by the proximal tubules by 5 min post-injection. Almost 90% of the injected dose is cleared via the renal system within 3 h of injection [41].

Other Imaging Agents

[^{99m}Tc]TcO_4^-

Pertechnetate ([^{99m}Tc]TcO_4^-) (Fig. 6a) is used in conjunction with other imaging agents—notably [^{99m}Tc]Tc-sestamibi and [^{201}Tl]TlCl—for the detection of thyroid cancer, via parathyroid scintigraphy [24, 34]. It is taken up by functional thyroid tissue through the Na^+/I^- symporter in a manner similar to iodide due to the similar ionic radii and charge [34, 45]. This pertechnetate "background" signal can be subtracted from the ^{99m}Tc-sestamibi or [^{201}Tl]TlCl scans to identify the diseased tissue corresponding to parathyroid carcinoma [24, 34].

[^{99m}Tc]Tc-Exametazime

[^{99m}Tc]Tc-Exametazime (Ceretec™) is an approved radiopharmaceutical used to detect altered regional cerebral perfusion in patients suffering from various cerebrovascular diseases [46, 47]. In addition, it can be used to label leukocytes for the localization of abdominal infections and inflammatory bowel disease [48]. [^{99m}Tc]Tc-Exametazime is a neutral Tc(V) complex of (RR,SS)-4,8-diaza-3,6,6,9-tetramethyl-undecane-2,10-dione bisoxime—a ligand commonly referred to as hexamethyl propylene amine oxime (HMPAO)—that exists as a mixture of D and L enantiomers (Fig. 6b). [^{99m}Tc]Tc-Exametazime is lipophilic and is thus able to cross the BBB, where it is converted by hydrolysis (at approximately 12% per hour) to a charged, hydrophilic complex that cannot recross the BBB, resulting in the intracerebral accumulation of the radiotracer [23, 46]. The activity concentration in the brain reaches a maximum of 3.5–7.0% of the injected dose within 1 min of injection, and up to 15% of the retained activity is cleared from the brain by 2 min after injection. Otherwise, moderate uptake is found throughout the body in muscle and soft tissue, with 50% and 40% of the injected dose being cleared via the hepatobiliary and renal systems, respectively.

[^{99m}Tc]Tc-DISIDA

[^{99m}Tc]Tc-DISIDA (diisopropyl iminodiacetic acid)—also known as [^{99m}Tc]Tc-disofenin (Hepatolite™)—is a metal complex of iminodiacetic acid that is used for imaging the hepatobiliary tract, gallbladder, and bile ducts (Fig. 6c) [49–51]. Prior to the advent of [^{99m}Tc]Tc-disofenin, another ^{99m}Tc-based radiopharmaceutical, [^{99m}Tc]Tc-dimethyl acetanilide iminodiacetic acid ([^{99m}Tc]Tc-HIDA), was used for these applications. The two radiotracers are derived from ligands that have the same group bound to ^{99m}Tc, though they differ structurally in the nature of the substituents. [^{99m}Tc]Tc-disofenin is currently used in a test that is anachronistically referred to as a "HIDA scan" [49, 50]. [^{99m}Tc]Tc-DISIDA

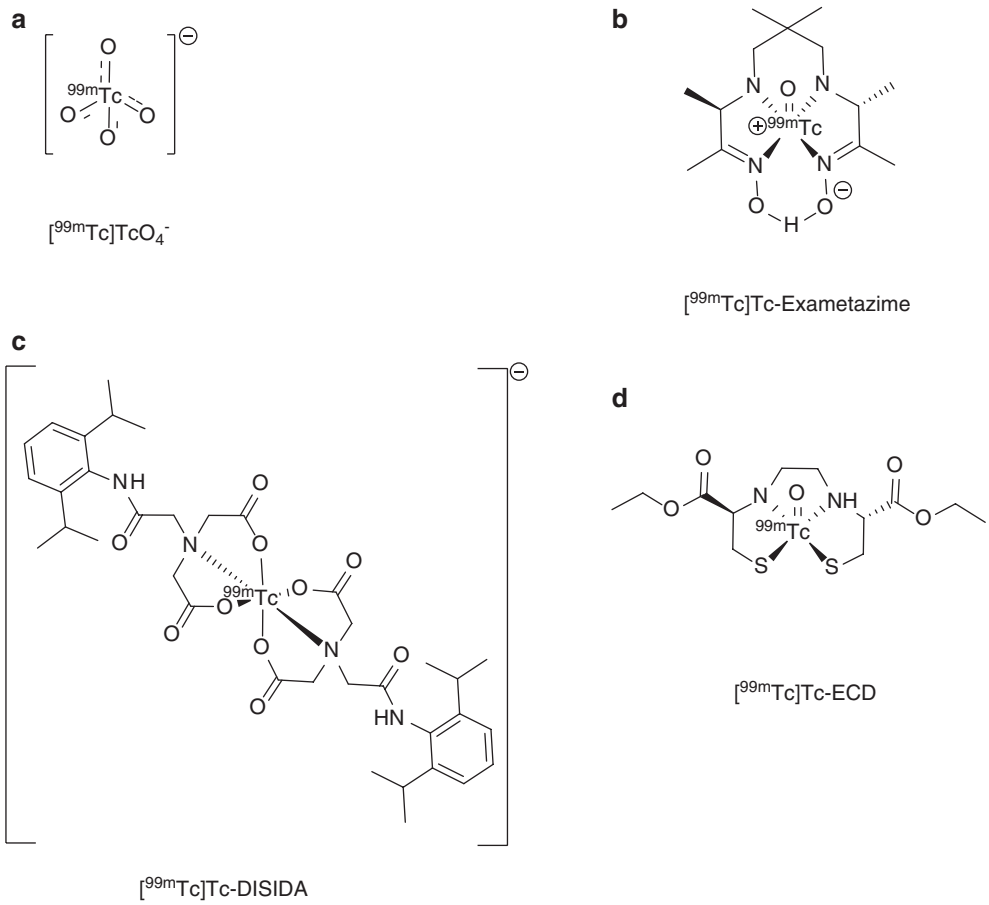

Fig. 6 Common ^{99m}Tc-labeled compounds used in nuclear medicine: (**a**) [^{99m}Tc]TcO_4^-, (**b**) [^{99m}Tc]Tc-exametazime, (**c**) [^{99m}Tc]Tc-DISIDA, and (**d**) [^{99m}Tc]Tc-ECD

is used for the diagnosis of gallbladder disease, as it rapidly clears from the liver to the gallbladder. The ^{99m}Tc complex binds to albumin resulting in decreased renal clearance and increased hepatic accumulation. Following uptake into the hepatocytes, the metal dissociates from the chelator. Patients are imaged for approximately 1 h following the administration of the radiotracer in order to track the production and flow of bile from the liver first to the gall bladder and then to the intestines [50, 51]. In the absence of gallbladder disease, the gallbladder is visualized within an hour; the lack of uptake in the gallbladder past 4 h is indicative of disease, the presence of gallstones, or the obstruction of the bile duct.

[^{99m}Tc]Tc-ECD

[^{99m}Tc]Tc-ECD (ethylene cysteine dimer; Neurolite™) is an approved radiopharmaceutical that is used for brain imaging in patients that have had a stroke [40, 52, 53]. This radiopharmaceutical is a stable and lipophilic complex that can pass through the BBB via passive diffusion. [^{99m}Tc]Tc-ECD is a neutral, square pyramidal complex containing a $[Tc(V)O]^{3+}$ core and a diaminedithiol ligand (Fig. 6d) [23]. The L,L stereoisomer crosses the cell membrane of brain cells in which it is metabolized via ester hydrolysis to create more polar and less diffusible compounds [52, 53]. If, on the other hand, the metal complex is hydrolyzed prior to crossing the BBB, the resulting metal-bound dicarboxylate anion is excreted via the renal system [23]. At 1 h post-injection, little activity remains in the blood. The uptake of [^{99m}Tc]Tc-ECD in the brain is cleared in a bi-exponential decay, with 40% of the activity being cleared with a 1.3-h half-life, and the remaining 60% cleared slowly with a half-life of 42.3 h [54]. By 2 h, 50% of the injected dose is cleared through the renal system, reducing background signals. SPECT imaging of the brain can begin 10 min following the administration of the radiotracer but should be performed 30–60 min postinjection to acquire optimal images [52]. The related complex, [^{99m}Tc]TC-ethylene dicysteine, [^{99m}Tc]Tc-EC, which is also a metabolite of [^{99m}Tc]Tc-ECD, is used to assess renal function and provides scintigraphy data equivalent to that obtained by [^{99m}Tc]Tc-MAG_3 [40]. [^{99m}Tc]Tc-EC is cleared through active tubular transport, allowing for the assessment of renal clearance in patients with suspected or known renal

failure. [^{99m}Tc]Tc-EC can be produced directly using an instant kit [40].

^{99m}Tc-Sulfur Colloid

^{99m}Tc can be used to label sulfur-based colloids to detect lymph node metastases associated with breast cancer as well as and to image peritoneovenous shunt patency, gastroesophageal reflux, and functional reticuloendothelial cells in the spleen, bone marrow, and liver [55, 56]. The product is obtained from a lyophilized mixture of anhydrous sodium thiosulfate, EDTA, and gelatin [55]. Mixing the contents of this kit with [^{99m}Tc]TcO_4^- and adjusting the pH with mixtures of NaOH and HCl results in the formation of the ^{99m}Tc-sulfur colloids for which the optimal size range is 15–100 nm [56]. ^{99m}Tc-sulfur colloid is administered differently depending on intended use. For lymphatic mapping, they are injected subcutaneously into the tissue surrounding the tumor [57]. When administered by intraperitoneal injection, ^{99m}Tc-sulfur colloid mixes with the peritoneal fluid, and its rate of clearance from the peritoneal cavity is used to evaluate peritoneovenous shunt patency [55]. When ^{99m}Tc-sulfur colloid is administered orally, it enters the gastroesophageal tract, allowing for gastric scintigraphy [55]. And finally, when administered intravenously, the uptake of the ^{99m}Tc-sulfur colloid in the reticuloendothelial system of the liver and spleen is dependent on the blood flow and the number and function of the phagocytic cells.

Tricks of the Trade: Practical Technetium Chemistry

The following section contains descriptions of selected practical procedures and calculations routinely used by researchers working with ^{99m}Tc. These were chosen by graduate students for new students interested in developing ^{99m}Tc radiopharmaceuticals.

Eluting a ^{99}Mo/^{99m}Tc Generator

To obtain [^{99m}Tc]TcO_4^- from a ^{99}Mo/^{99m}Tc generator, a sealed vial containing 0.9% (9 mg/mL) saline is placed on the inlet needle at the top of the generator (see Fig. 1b(c)). Next, an evacuated vial (which often comes with the generator) is situated in a lead container and placed on the collection inlet needle (see Fig. 1b(d)). Once the needle has pierced the collection vial, the saline from the stock vial will travel through the generator "carrying" the [^{99m}Tc]TcO_4^- into the collection vial. Once emptied, the saline vial can be removed followed by the collection vial. At this point, the needles should be wiped with a tissue or a suitably absorbent material held using tweezers, making sure to wipe the saline needle first. The storage caps should then be placed on the inlet needles until the next elution, and the amount of activity in the sample measured using a dose calibrator.

Determining the Mass of ^{99m}Tc

Understanding the amount of material you are working with when labeling compounds is a critical part of radiochemistry. To determine the amount of technetium in a sample, you simply need to know the half-life of the radionuclide and the amount of activity present in the sample. A sample calculation shown in Fig. 7a highlights the relationship between half-life, activity, and the amount of material in a sample. Another widely used term is specific activity (A_s), which is the amount of activity per unit of mass of a sample [23]. A_s is typically expressed in Ci/g or Bq/g, and a sample calculation for the specific activity in a 3.7×10^8 Bq sample of [^{99m}Tc]Tc-MDP is shown in Fig. 7b. Note that there is another term, effective specific activity, which is defined as the specific activity divided by the amount of ligand present in the sample. This is a critical factor which is often erroneously used interchangeably with specific activity. For targeted radiopharmaceuticals, the presence of too much unlabeled ligand can result in competition between the said ligand and the radiotracer for binding to the target. On the other hand, however, effective specific activities that are *too* high can result in nonspecific binding and low uptake at the desired target or a compound that has poor stability (*e.g.* [^{99m}Tc]Tc-MDP) [23].

The Preparation of ^{99m}Tc Complexes

The predominant method for the preparation of ^{99m}Tc-based radiopharmaceuticals is to combine [^{99m}Tc]TcO_4^- with a reducing agent and a suitable ligand [58]. The yield and nature of the product are greatly influenced by several factors, including the identity and concentration of the ligand, the identity and concentration of the reducing agent, temperature, and pH. As discussed previously, a wide array of ligands and labeling conditions have been reported for the synthesis of ^{99m}Tc complexes, and a selection of commonly used methods is provided below [6, 59–62]. Note that when preparing novel ^{99m}Tc complexes, graphs of yield versus key factors (*e.g.* pH, temperature, ligand concentration, time, *etc.*) should be generated to help identify the optimal labeling conditions.

Tc(V) Complexes of Hydrazinonicotinic Acid (HYNIC)

One of the more prevalent oxidation states of ^{99m}Tc in radiopharmaceuticals is ^{99m}Tc(V). Here, stannous chloride ($SnCl_2$) has proven to be an effective and biocompatible reducing

a

$$\text{half life} = \tau_{1/2} = \frac{\ln 2}{\lambda}$$

$$\text{Decay Constant} = \lambda = \frac{\ln 2}{21600\,\text{sec}}$$

$$= 3.2 \times 10^{-5}\,{}^{1}\!/_{\text{sec}}$$

$$\text{Activity in Sample} = A = 10\,\mu\text{Ci}$$

$$1\text{Ci} = 3.7 \times 10^{10}\,\text{Bq}$$

$$A = 10\,\mu\text{Ci} = 1.0 \times 10^{-5}\,\text{Ci}/3.7 \times 10^{10}$$

$$= 3.7 \times 10^{5}\,\text{Bq}$$

$$A = N\lambda$$

$$\text{Number of moles} = N = \frac{A}{\lambda}$$

$$= \frac{3.7 \times 10^{5}\,\text{Bq}}{3.2 \times 10^{-5}\,{}^{1}\!/_{\text{sec}}}$$

$$= 1.2 \times 10^{10}$$

$$\text{Moles} = n = \frac{N}{N_A}$$

$$= \frac{1.2 \times 10^{10}}{6.022 \times 10^{23}}$$

$$= 1.99 \times 10^{-14}\,\text{mol}$$

$$= 0.02\,\text{pmol}$$

b

$$\lambda = \frac{\ln 2}{\tau_{\frac{1}{2}}}$$

$$= \frac{\ln 2}{21600\,\text{sec}}$$

$$= 3.2 \times 10^{-5}\,{}^{1}\!/_{\text{sec}}$$

$$A = N\lambda$$

$$\text{Activity} = 10\,\text{mCi} = 3.7 \times 10^{8}\,\text{Bq}$$

$$N = \frac{A}{\lambda}$$

$$= \frac{3.7 \times 10^{8}\,\text{Bq}}{3.2 \times 10^{-5}\,{}^{1}\!/_{\text{sec}}0}$$

$$= 1.2 \times 10^{13}$$

$$n = \frac{N}{N_A}$$

$$= \frac{1.2 \times 10^{13}}{6.022 \times 10^{23}}$$

$$= 1.99 \times 10^{-11}\,\text{mol}$$

$$m = n \times MW_{\text{Tc-MDP}}$$

$$= 1.99 \times 10^{-11}\,\text{mol} \times 274.907\,{}^{\text{g}}\!/_{\text{mol}}$$

$$= 5.47 \times 10^{-9}\text{g}$$

$$\text{Specific Activity} = A_s = \frac{A}{m}$$

$$= \frac{3.7 \times 10^{8}\,\text{Bq}}{5.47 \times 10^{-9}\,\text{g}}$$

$$= 1.83 \times 10^{6}\,\text{Bq/g}$$

Fig. 7 Example calculations for ^{99m}Tc-labeled compounds. (**a**) Sample calculation showing the amount of ^{99m}Tc in 10 μCi and (**b**) sample calculation showing the theoretical specific activity of [^{99m}Tc]Tc-MDP

agent for the conversion of pertechnetate into ^{99m}Tc(V) complexes. As a result, $SnCl_2$ is currently used in several kits for the commercial production of [^{99m}Tc]Tc-DMSA, [^{99m}Tc]Tc-ECD, [^{99m}Tc]Tc-DTPA, [^{99m}Tc]Tc-exametazine, and [^{99m}Tc]Tc-tetrofosmin [30, 36, 39, 46, 52, 63].

The reduction of [^{99m}Tc]TcO_4^- with $SnCl_2$ in the presence of bifunctional ligands and their biomolecular conjugates has also been widely used to prepare targeted radiopharmaceuticals. For example, hydrazinonicotinic acid (HYNIC) readily forms stable complexes with ^{99m}Tc(V) and, as a result, was developed as a convenient way to introduce a ^{99m}Tc-binding chelating group into proteins and peptides [64]. As HYNIC does not occupy the entire coordination sphere of the metal, co-ligands such as tricine and ethylenediamine diacetic acid are often added to radiolabeling reactions involving HYNIC-bearing bioconjugates [65, 66]. Methods for the conjugation of HYNIC to biomolecular vectors have been well established in the literature and typically rely upon the use of a bifunctional variant of HYNIC that has an amine-reactive functionality. Once prepared, typical labeling conditions involve the incubation of the HYNIC ligand (3–100 μg), a co-ligand (5–50 mg), and stannous chloride (50–200 μg) for 15–30 min either at room temperature (for sensitive proteins) or 100 °C (for thermally robust molecules) [64, 66–70]. HYNIC labeling yields are generally high, and impurities can be identified using iTLC or HPLC [64, 67].

[^{99m}Tc][Tc(CO)$_3$]$^+$ Complexes

[^{99m}Tc]Tc(I) complexes have also become commonplace in the literature as a result of the ease with which a unique organometallic precursor—[^{99m}Tc][Tc(CO)$_3$(H$_2$O)$_3$]$^+$—can be prepared from pertechnetate in aqueous solutions [71–73]. This synthon is highly useful not only because the carbonyl ligands create a remarkably stable complex but also because the water ligands can be replaced by a variety of donor groups, enabling the formation of a large number of different Tc(I) complexes [17, 74–79]. [^{99m}Tc][Tc(CO)$_3$(H$_2$O)$_3$]$^+$ is formed via the reaction of [^{99m}Tc]TcO_4^- and potassium boranocarbonate ($K_2[BH_3CO_2]$), which acts as both a reducing agent and a source of carbonyl ligands. In the presence of the appropriate buffers, high yields of [^{99m}Tc]

$[Tc(CO)_3(H_2O)_3]^+$ can be obtained in a single step (Table 2). In order to reduce the time required for preparation, these reagents can also be heated in a microwave following purging with argon for 10 min. It is important to note that only a microwave approved for laboratory use should be employed [71, 72, 75, 80–82]. This microwave procedure facilitates the formation of $[^{99m}Tc][Tc(CO)_3(H_2O)_3]^+$ in quantitative yields in only 3.5 min when the reaction is performed at 110 °C [72]. After the reaction is complete, the pH of the $[^{99m}Tc][Tc(CO)_3(H_2O)_3]^+$ solution should be adjusted using 1 M HCl since the reaction solution is highly basic.

Table 2 Roles of each reagent in the preparation of $[^{99m}Tc]Tc[(CO)_3(H_2O)_3]^+$

Reagent	Role
Potassium boranocarbonate ($K_2[BH_3CO_2]$)	Reducing agent, solid source of CO
Sodium carbonate (Na_2CO_3) and sodium tetraborate decahydrate ($Na_2B_4O_7{\cdot}10H_2O$)	Buffers, where optimal pH is 8.0.
Potassium sodium tartrate $KOCO[CH(OH)]_2COONa{\cdot}4H_2O$	Stabilizes ^{99m}Tc-complexes of intermediate oxidation states

$K_2[BH_3CO_2]$—first reported by Alberto and colleagues—is a critical component for the preparation of complexes containing the $[^{99m}Tc]Tc[(CO)_3]^+$ synthon [83]. The experimental setup used to prepare this unique reagent is shown in Fig. 8. First, carbon monoxide gas is passed through 1 M KOH and subsequently a column containing a calcium sulfate drying agent to remove any residual water (flask A). The gas is then passed into a solution of 1.0 M $BH_3{\cdot}THF$ (flask B) which is cooled in an ice bath to 0 °C and connected to an ammonia condenser that is cooled to −60 °C using dry ice in acetone. The ammonia condenser allows for the THF to be condensed and remain in flask B, while the gaseous $BH_3{\cdot}CO$ can travel to flask C, where it is passed through a solution of KOH in ethanol for 5 h at −80 °C to produce $K_2[BH_3CO_2]$, which precipitates from the solution. The solution is allowed to warm to room temperature, and $K_2[BH_3CO_2]$ is collected by filtration and washed with cold ethanol. The isolated $K_2[BH_3CO_2]$ is then dried under vacuum, leaving a white solid which can be stored at room temperature and used for several months. Prior to the preparation of this material, readers should refer to the original publications for important details regarding the method and hazards [72, 75, 79, 83].

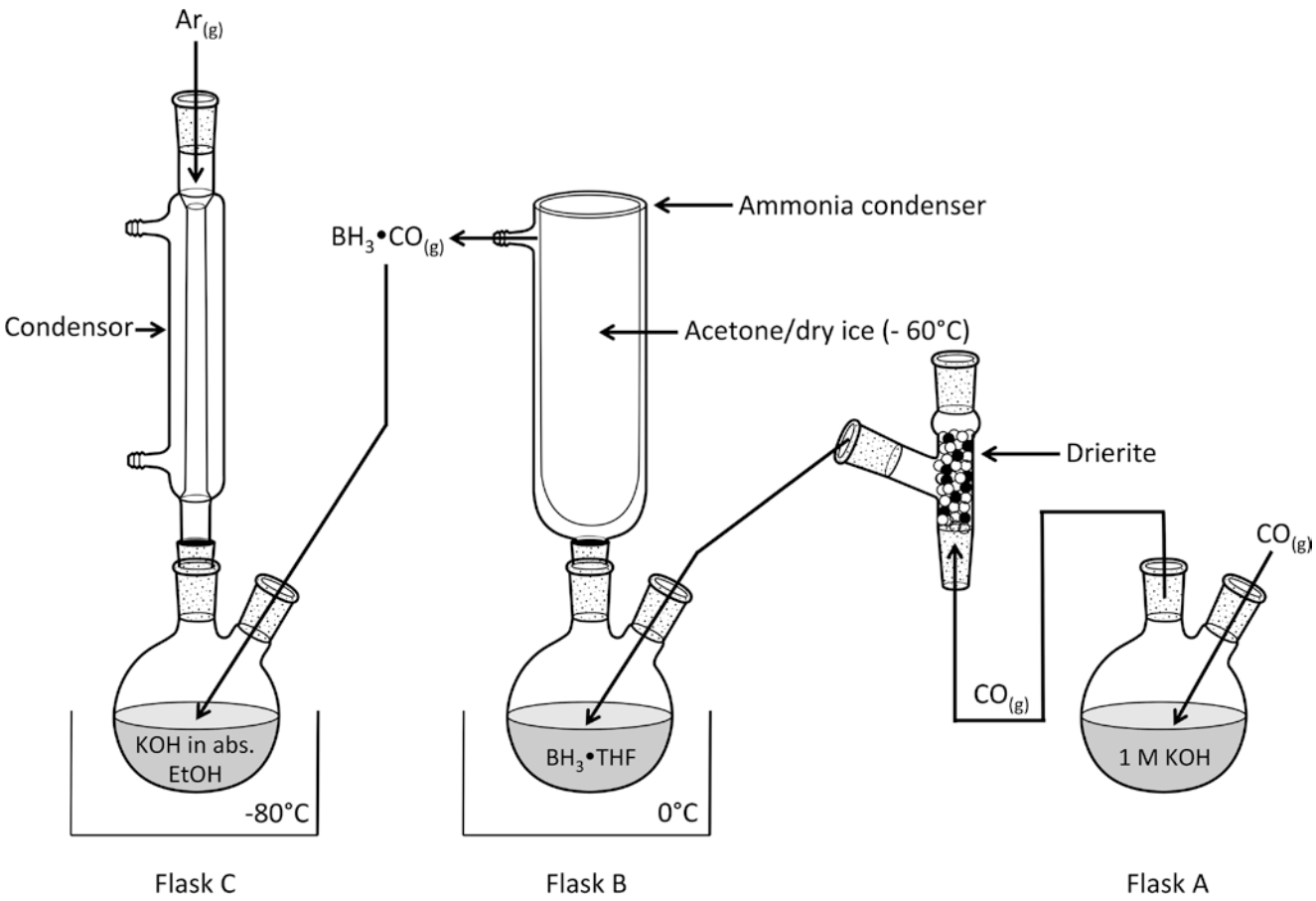

Fig. 8 Reaction setup for the synthesis of $K_2[BH_3CO_2]$

Preparing ^{99m}Tc Compounds for Biodistribution Studies

Once a ^{99m}Tc complex has been prepared, there are several studies that should be performed prior to assessing the performance of the complex *in vivo*. First, the purity of the ^{99m}Tc-labeled complex must be confirmed using HPLC and radio-TLC, and the structure of the product should be verified, preferably using a fully characterized rhenium (or ^{99}Tc) reference standard. When determining the purity of a ^{99m}Tc complex by HPLC, it is important to use two different elution methods or columns. Ideally, the compound should have a radiochemical purity greater than 95%, with no single impurity in an abundance higher than 1%. Once the optimal radiosynthesis conditions have been determined and the desired product obtained, the yield and reproducibility of the synthesis for the ^{99m}Tc complex should be assessed using a minimum of three independent labeling experiments. If yields vary by more than 5–10%, the conditions should be further optimized to ensure the robustness of the reaction.

Two common impurities that can form during the preparation of ^{99m}Tc complexes are $[^{99m}Tc]TcO_4^-$ and colloidal $[^{99m}Tc]TcO_2$. The latter is often a result of conditions in which the ligands do not form adequately stable complexes with ^{99m}Tc, the ligands are poorly soluble, or the amount of the ligand and reducing agent is not optimal. Residual $[^{99m}Tc]TcO_4^-$ can result from cases in which insufficient amounts of the reducing agent have been added, the reducing agent decomposes, or the metal complex itself decomposes. The quality of the reducing agent should be checked if labeling yields are low or highly variable. RadioTLC is a convenient way to identify the presence of colloidal $[^{99m}Tc]TcO_2$ and $[^{99m}Tc]TcO_4^-$ [31]. A simple procedure to assess the presence of both compounds is provided in Table 3.

Once the purity and nature of a ^{99m}Tc-labeled compound have been confirmed, the product must be formulated in an appropriate biocompatible solvent (*e.g.* 0.9% saline, PBS) prior to administration to a test animal. Solvents should be pharmaceutical grade and preferably passed through a microporous filter (0.2 μm) before use. A general checklist for formulating a compound for testing in preclinical models is provided in Fig. 9a. However, additional regulations regarding formulation may be also required by an institution's animal ethics committee.

Table 3 TLC conditions for the separation of chelate complexes of ^{99m}Tc, $[^{99m}Tc]TcO_2$ colloid and $[^{99m}Tc]TcO_4^-$

TLC plate	Eluent	Location of $[^{99m}Tc]TcO_2$ colloid	Location of $[^{99m}Tc]TcO_4^-$	Typical location of ^{99m}Tc-chelate
iTLC-SG glass microfiber chromatography paper	Acetone	Baseline	Solvent front	Baseline
	Distilled water	Baseline	Solvent front	Solvent front

Because of the small molar amounts of material being handled, ^{99m}Tc-labeled complexes can adhere to surfaces. As a result, adhesion ("stickiness") testing should also be performed to ensure that novel ^{99m}Tc-compounds do not bind to surfaces, including—and most frustratingly—the syringe at the time of injection. To test this, the optimal formulation and concentration of activity for injection should be drawn into the exact type of syringe to be used during the administration of the radiopharmaceutical to the animal. Ideally, this should be done in triplicate, with the activity in each syringe measured in a dose calibrator and the volume and amount of activity recorded. The dose should then be dispensed into a vial, and the residual activity in the syringe and vial should be measured. The amount of activity remaining in the syringe should be less than 10% of the total activity. If the amount of activity in the syringe is >10%, the formulation should be adjusted accordingly. There are several options available for reducing adherence, including the addition of a surfactant (*e.g.* Polysorbate 80), 0.5% BSA, or a small amount of a biocompatible solvent (*e.g.* 1–5% ethanol, 0.1–2% DMSO).

Once the final formulation has been determined, the next step is to perform stability testing. This requires incubating the complex in the formulation solution at 37 °C for up to 24 h and checking the purity of the sample at various time points using either iTLC or HPLC. The fraction of intact compound should be calculated at each time point to determine the rate of the decomposition process. The time between formulation and injection should not exceed a window during which the compound remains ≥95% pure.

The lipophilicity of the compound should also be measured. The lipophilicity of a new imaging agent is an important aspect in predicting and understanding its absorption and binding to plasma proteins as well as in guiding the further optimization of its pharmacokinetics [84]. The log *P* value of a compound is a measure of its partition coefficient between water and 1-octanol and can be calculated using the "shake flask" method [84]. In this method, equal amounts of the ^{99m}Tc complex are dissolved in three vials containing equal parts 1-octanol and water, and these vials are placed on a shaker for 20 min. Following the agitation, the vials are centrifuged, and fractions are taken from each layer and transferred to pre-weighed tubes suitable for use in a gamma counter. The log *P* value for the compound can then be calculated by dividing the mass of the solution in each of the tubes by the counts per minute (CPM) values obtained from a gamma counter. Note that it is important to follow the detailed procedure described in the paper by Wilson *et al.* [82, 84] in order to understand the limitations of the method and to ensure reproducible and accurate results.

Given that there are endogenous ligands that can promote the transmetalation of ^{99m}Tc from a radiopharmaceutical,

a

- ❑ Removal of all non-biocompatible salts
- ❑ Removal of all non-biocompatible solvents
- ❑ Prepared in sterile biocompatible solvent (i.e. saline, PBS)
- ❑ Contain less than 10% EtOH, or 1% DMSO in final formulation (if appropriate)
- ❑ Ensure pH is within the range 6-8
- ❑ Osmolality should be >450 mOsm/kg

b

- ❑ Mouse/small animal restraint device and/or anesthetic machine
- ❑ Alcohol wipes
- ❑ 30 gauge needles (2 per mouse)
- ❑ 25 gauge needles (2 per mouse)
- ❑ 1 ml polycarbonate syringes (2 per mouse)
- ❑ Lead containers for transport of ^{99m}Tc complexes
- ❑ Dose calibrator, calibrated for ^{99m}Tc
- ❑ Gamma counter, set for ^{99m}Tc
- ❑ Gamma tubes with caps and tube racks (one tuber per organ/tissue, per mouse, pre-weighed and recorded)
- ❑ Analytical balance
- ❑ 2 sets of forceps (1 fine tip, 1 regular tip)
- ❑ 1 pair of surgical scissors
- ❑ 1 beaker of PBS (for rinsing tissues/organs)
- ❑ Paper towels
- ❑ Anesthetic (i.e. isoflurane, ketamine, etc.)
- ❑ Oxygen tank or medical air
- ❑ Documentation records (notebooks with tables) prepared in advance

Fig. 9 Practical checklists for *in vivo* studies. (**a**) Checklist for formulating a compound for testing in preclinical models and (**b**) checklist of standard equipment and supplies required for a biodistribution study

ligand challenge experiments are also valuable when developing novel ^{99m}Tc-based agents. Two common tests are the cysteine and histidine challenges, in which the purified and formulated ^{99m}Tc complex is incubated separately with 2 mM cysteine or 2 mM histidine—the approximate concentration of these ligands in the blood—in PBS (pH 7.4) at 37 °C, typically for 6 h [85]. The stability of the ^{99m}Tc complex can be monitored at selected time points (typically hourly) using HPLC or iTLC [75, 86]. The appearance of new peaks and changes in retention time or peak shape versus that of the purified ^{99m}Tc complex would suggest that the metal complex may not have adequate stability for use *in vivo*.

For targeted radiopharmaceuticals, the next step is typically *in vitro* cell binding studies. The goal here is to test the ability of new ^{99m}Tc complexes to bind to a specific target that is overexpressed as a result of disease or injury. Although the experimental aspects of these studies vary depending on the nature of the target and targeting ligand, a commonly used approach involves the incubation of the formulated ^{99m}Tc complex with a cell line that overexpresses the target of interest. As a control to ensure binding is not due to non-specific, non-selective, or off-target binding, blocking studies are performed with increasing concentrations of a ligand that is known to bind the target of interest. Alternatively, substitution of the cell line for one that does not express the target can also be used as a control.

Biodistribution Studies

Once all of the appropriate formulation, stability, and *in vitro* testing studies have been completed, biodistribution and imaging studies can be performed. For the former, several time points will be needed to get an accurate picture of

the pharmacokinetic profile of the radiopharmaceutical, and multiple animals per time point are required to ensure reproducibility and address biological variability. The number of animals needed per study depends on the robustness of the model being used but typically lies between three and five animals per time point (see the chapter on "An Introduction to Biostatistics") [87]. With respect to timing, an early time point (5–30 min) should be taken to observe the initial distribution of the tracer as well as the activity concentration in the blood. Intermediate time points (1–2 h) should also be used to determine the clearance pathways, and finally, a later time point at least one half-life (6 h) following the administration of the tracer should be employed as well. However, the signal to background noise may not always be ideal at 6 h, so later time points such as 12 and 24 h can also be used, provided there is adequate activity remaining in the organs of interest.

The choice of animal model to evaluate new radiopharmaceuticals is a complex issue that requires careful consideration (see the Chapters on "Preclinical Experimentation in Oncology" and "Preclinical Experimentation in Neurology"). Once the ideal model has been chosen, it is important to realize that in the weeks leading up to a biodistribution study, the animals may need a specific diet (*e.g.* high fat, fasting, etc.) or other regimens to yield reproducible and representative results. All animal care and preparation should be in accordance with the animal care and use protocols of the research institution where the studies are performed. It is almost impossible to be *too* prepared for a preclinical biodistribution study. This is particularly true for scientists new to this field. Before beginning, it is essential to prepare materials akin to what is done in an operating room. A list of standard equipment and supplies for a biodistribution study can be found in the checklist in Fig. 9b. Students who are new to the field should consider repeating a biodistribution study of a known radiopharmaceutical (*e.g.* ^{99m}Tc-sestamibi) prior to working with an experimental agent, in order to ensure that their procedures and techniques are robust [88].

On the day of a biodistribution study, doses of the formulated ^{99m}Tc complex should be prepared along with standards for the gamma counter and dose calibrator. It is important to note that when labeling and purifying a ^{99m}Tc complex, excess radiopharmaceutical should always be prepared, because standards are certainly necessary and backup doses may be needed in the event of a problem. For the dose calibrator standard, the volume equivalent of a single dose should be used, and the activity of the standard and time of measurement should both be recorded. When preparing the gamma counter standards, small aliquots from the stock solution should be used (~18.5–37 kBq; 0.5–1 μCi) so as to not saturate the gamma counter. Replicates (typically 4–6) of the gamma standard should be prepared and measured to determine an average count value per unit of activity. The volume of the standards used should be recorded. It is also important to ensure that the gamma counter has been properly calibrated, that the dose calibrator has been maintained according to the manufacturer's directions, and that the limits of detection and linear dynamic ranges are known for both instruments.

When preparing doses, each dose should be placed in a separate syringe fitted with a new needle; a reused needle can quickly dull and make injections difficult. When drawing up a dose, it is also imperative to ensure that there are no air bubbles in the syringe or needle hub. The injection volume should be no more than 20% of the total blood volume of the mouse. A formula for calculating the blood volume of a mouse as a function of its weight is shown below, where 0.049 is the percent of total body mass attributed to the blood [89].

$$\text{Blood volume}(\text{mL}) = \text{body weight}(\text{g}) \times 0.049$$

At the chosen time points for the biodistribution study, the mice of each cohort should be euthanized according to the protocols outlined by the institution where the experiment is being performed [72]. Subsequently, the blood of the mice can be collected via cardiac puncture, and the other organs and tissues can be removed, washed in saline or PBS, and dried before transfer to pre-weighed tubes for gamma counting. The weight of each filled tube should then be recorded, and then the tubes containing the organs, tissues, and standards can be loaded onto the gamma counter. Following the counting of the samples, the gamma counter will print or display the counts from each gamma tube, typically reported as counts per minute (CPM). Measuring the gamma counter standards at the same time as the organs and tissues removes the need for decay correction, as this correction will be integrated into the CPM/μCi calculation. After determining the average CPM values for the standards, the volume of the dose calibrator standard should be divided by the volume of the gamma counter standard. Using these calculated values and the activity of the dose calibrator standard, the following formula can be used:

$$\frac{(\text{Average gamma standard CPM}) \times \left(\dfrac{\text{volume dose cal standard}}{\text{volume gamma standard}} \right)}{\text{Dose cal standard activity}} = \frac{\text{CPM}}{\mu\text{Ci}}$$

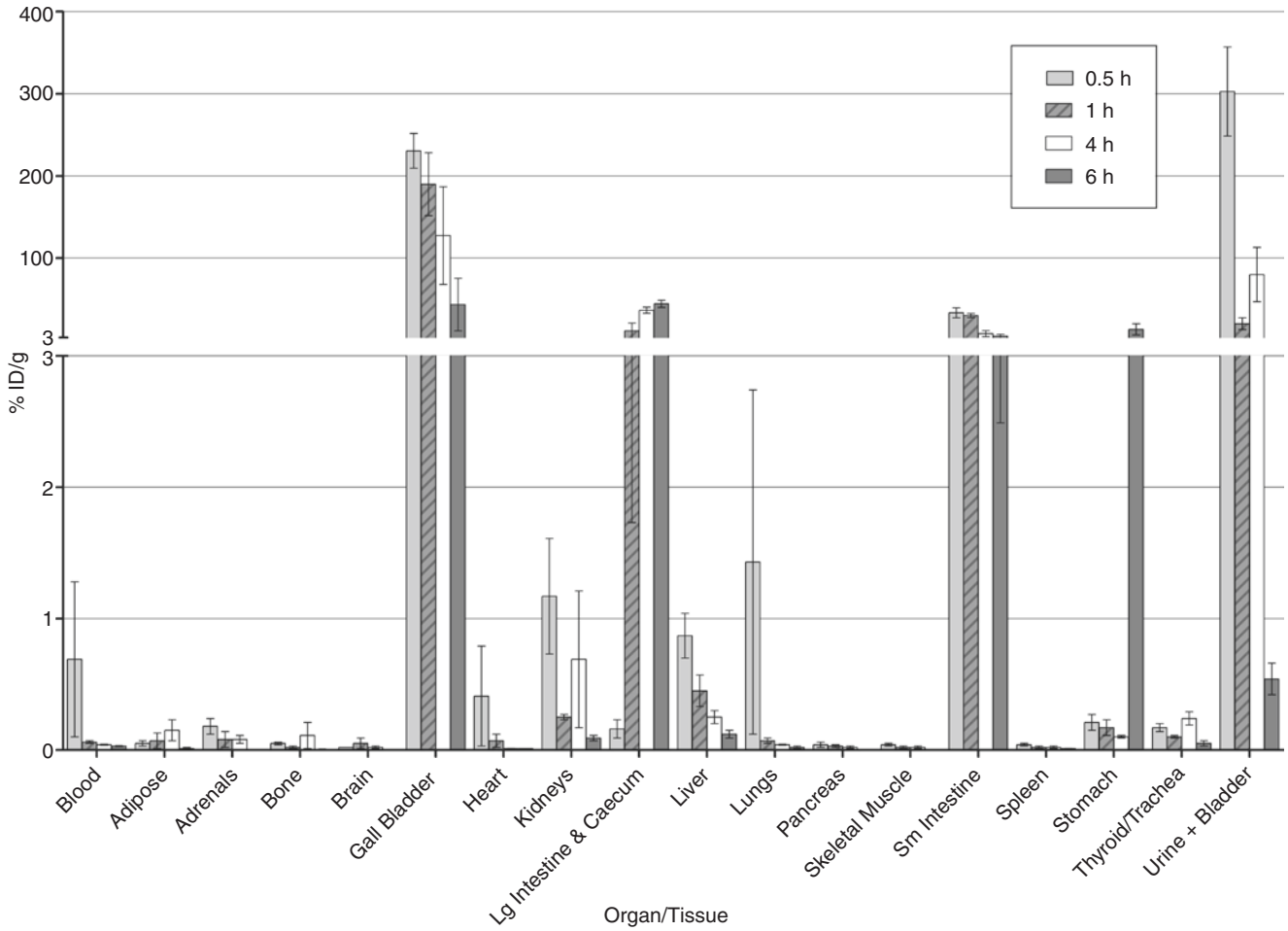

Fig. 10 Example biodistribution study results. Typical graph of biodistribution data. These results were for a ^{99m}Tc-labeled tetrazine, and the animals (Balb/c mice) were sacrificed at 0.5, 1, 4, and 6 h post-injection (n = 3 mice). Activity was normalized to the weight of various tissues or fluids (x-axis), as mean percent injected dose per gram of tissue or fluid (%ID/g) ± SEM (y-axis) (From Bilton *et al.* [72], with permission)

Using this calculated value, the raw CPM values of each organ/tissue can be converted to μCi/organ

$$\frac{\text{Organ CPM value}}{\text{Standard CPM / μCi}} = \text{μCi / organ}$$

After obtaining these values, the amount of activity can then be divided by the total activity injected, giving the percent injected dose (%ID) per organ. This value can further be divided by the mass of each tissue, organ, or fluid to give the normalized value reported as %ID/g.

When reporting biodistribution data, graphs of the %ID/g and the %ID per tissue/fluid are typically generated (Fig. 10). The former is especially important, as it gives a sense of the amount of activity normalized to the weight of the organ/tissue. Note also that high and unexpected activity concentrations in the liver, lung, and spleen can indicate the presence of colloidal [^{99m}Tc]TcO_2 [90]. In contrast, the presence of [^{99m}Tc]TcO_4^-—which can be the result of poor labeling yields or decomposition—can produce high activity concentrations the stomach and thyroid.

Bifunctional Chelators and the Importance of Optimized Pharmacokinetics for Creating Next-Generation Targeted ^{99m}Tc Radiopharmaceuticals

Bifunctional Chelators for Developing Targeted ^{99m}Tc Radiopharmaceuticals

One would expect that the ideal nuclear properties, low cost, and prevalence of ^{99m}Tc would make it the leading medical radionuclide for the creation of new radiopharmaceuticals [91]. However, other diagnostic radionuclides—notably ^{18}F, ^{68}Ga, and ^{89}Zr—are playing a greater role in this regard. The reasons for this are multifaceted, but one major issue is

the difficulty in linking ^{99m}Tc to biomolecular targeting vectors without having a detrimental influence on the *in vivo* distribution of the parent biomolecule itself.

While a number of innovative strategies for labeling targeted vectors with ^{99m}Tc have been developed, none have become widely available in the clinic. When considering the development of new ^{99m}Tc-based radiopharmaceuticals, the design and optimization of the ligands for ^{99m}Tc are critical considerations. Much can be learned from work done on chelators for Tc(V) and Tc(I). For example, knowledge gained from the study of ^{99m}Tc(I) complexes was ultimately used to create a radiopharmaceutical for imaging the expression of prostate specific membrane antigen (PSMA) [81].

Chelators for Tc(V)

N_xS_y Tetradentate Chelators

Over the past several decades, there has been a tremendous body of work on developing bifunctional tetradentate chelators for Tc(V). These include mixed amine- and thiol-based chelators (N_xS_y, x + y = 4), most notably N_2S_2 [*e.g.* bis(aminoethanethiol) (BAT)] and N_3S [*e.g.* mercaptoacetylglycylglycylglycine (MAG_3)] variants (Fig. 11a, b) [62]. These ligands are extremely efficient at forming ^{99m}Tc complexes, and their radiometalation can be performed via a ligand exchange reaction with [^{99m}Tc]Tc-glucoheptonate or through direct reduction of pertechnetate. For example, technetium-labeled BAT complexes have been used to image targets in the brain, as they are capable of crossing the blood-brain barrier. ^{99m}Tc-labeled MAG_3 compounds, in contrast, can be used to prepare targeted radiopharmaceuticals and, as noted previously, to assess kidney function (see Fig. 11b) [42]. While substituted analogues of these ligands have been reported, these variants often form isomers, which can hinder translation because it may be necessary to assess the *in vivo* properties of each isomer (see Fig. 2).

Hydrazinonicotinamide (HYNIC)

HYNIC ligands were created as a convenient method for radiolabeling biomolecules with ^{99m}Tc (see the section on "The Preparation of ^{99m}Tc Complexes"). The active ester of HYNIC can readily be conjugated to small molecules and proteins, and the hydrazine donor can form a stable metal-nitrogen multiple bond complexes with ^{99m}Tc [60]. To occupy the remaining coordination sites, HYNIC—which can act as a monodentate ligand or a bidentate ligand with the added coordination of its pyridine nitrogen—requires co-ligands. These co-ligands create a convenient handle for fine-tuning the pharmacokinetic properties of the imaging agent by varying the polarity and charge of the additional ligands (Fig. 11c). A wide range of biomolecules have been labeled with HYNIC, but none have yet made it to routine clinical use. The reason for this lack of success remains unclear; however, it may be due to the absence of an optimal co-ligand.

Chelators for Tc(I)

As we have discussed, [^{99m}Tc][$Tc(CO)_3(H_2O)_3$]$^+$ can be used to prepare a wide range of chelator complexes via the substitution of the labile water ligands. Numerous examples of bidentate and tridentate chelators have been reported, including bifunctional derivatives that can be linked to targeting molecules [59, 92–94]. Tridentate chelators bearing nitrogen, oxygen, and sulfur donor groups and featuring a range

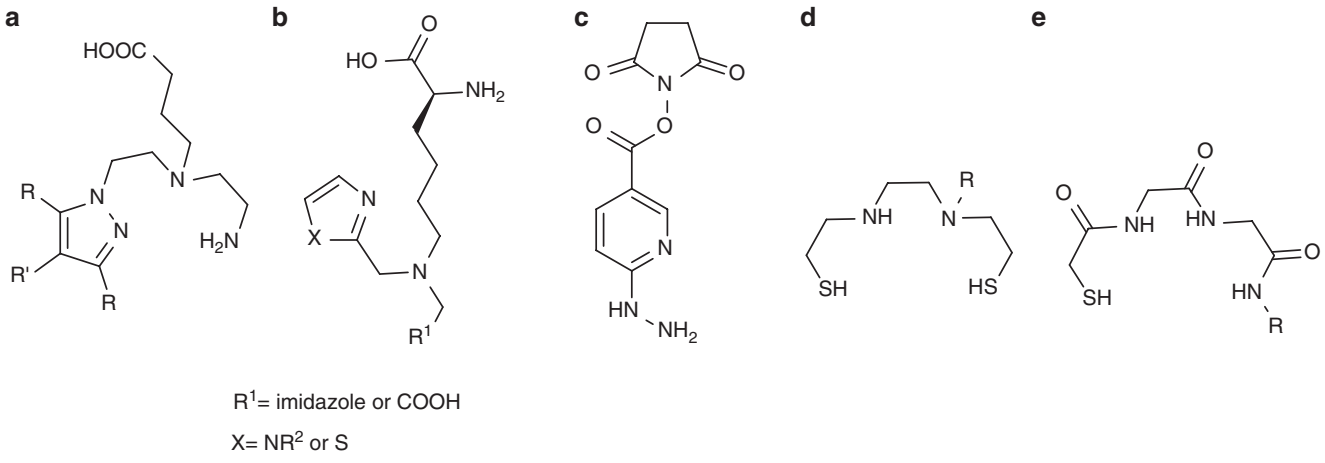

Fig. 11 Structures of different technetium chelators. (**a**) Pyrazole derivatives [94]; (**b**) single-amino-acid chelators [59]; (**c**) HYNIC [60]; (**d**) BAT [62]; and (**e**) MAG_3 [43]

of different heterocycles including pyridines, triazoles, imidazoles, and pyrazoles have been reported (see Fig. 11).

This chemical technology has been used to create many ^{99m}Tc(I)-based radiopharmaceuticals. Raposinho and colleagues, for example, designed a technetium probe to image the melanocortin-1 receptor through the functionalization of a peptidic α-melanocyte-stimulating hormone [94]. A cyclic peptide was synthesized and labeled with the $[^{99m}Tc][Tc(CO)_3]^+$ core through a variety of functionalized pyrazole-diamine chelators. Four pyrazole derivatives were tested, and it was found that the addition of a carboxylate group on the pyrazole ring significantly reduced the uptake of the imaging agent in the kidneys and liver compared to the parent compound (see Fig. 11a). More specifically, the addition of the carboxylate acid groups decreased the activity concentrations in the kidneys and liver by more than 89% and 91%, respectively, clearly demonstrating the sensitivity of these constructs to subtle changes in the structure of the chelator.

In analogous work, Pomper and coworkers synthesized a library of PSMA-targeted compounds and evaluated their uptake in murine models of prostate cancer [92]. The authors synthesized chelators based on quinolone and pyridine, and the ^{99m}Tc complex of the former suffered from high uptake in the liver. The pyridine derivatives, on the other hand, resulted in better clearance profiles, and their pharmacokinetic profiles were further improved by changing the nature of the spacer between the targeting molecule and the chelator.

It is undeniably time-consuming to synthesize a library of different chelators with various linker groups in order to optimize the pharmacokinetics of a ^{99m}Tc-labeled radiopharmaceutical. Nonetheless, when creating ^{99m}Tc-based imaging agents, it is important to ensure that the synthetic methods allow for the introduction of structural variations. For example, click chemistry has been used as a convenient means to create libraries of structurally diverse chelators for Tc(I) (Fig. 12) [6]. In this system—in which the additional two donor atoms are present on the molecule containing the alkyne—the N3 of the triazole ring coordinates the metal. This is termed a "regular" click ligand. If, one the other hand, the donor groups are on the azide, the N2 of the triazole will coordinate the metal. This, not surprisingly, is called an "inverse" click ligand. Both variants are easily synthesized and can be used to produce a variety of different chelators. However, it is important to note that the radiolabeling chemistry of these two constructs is different. For instance, "inverse" click ligands require 10^{-3}–10^{-2} M ligand to achieve quantitative labeling, while "regular" click ligands need only 10^{-5}–10^{-6} M. Moreover, ^{99m}Tc-labeled variants of bombesin bearing "inverse" click ligands showed reduced *in vivo* stability relative to analogues containing "regular" click ligands [6]. Mindt, Schibli and coworkers further exploited the "click-to-chelate" concept to prepare a variety of chelators through the use of functionalized L-propargylglycine and L-azido alanine [93].

Amino acids have also been widely used to introduce structural diversity into chelators for ^{99m}Tc(I) as well as help optimize the pharmacokinetic properties of bioconjugates [59]. For example, a class of compounds known as single amino acid chelators (SAACs) was developed using a lysine backbone that can be easily modified to introduce different heterocycles as donor groups (see Fig. 11b). These compounds are easy to prepare, and the products form robust complexes with Tc and Re in high yield. Unfortunately, the first generation of SAAC ligands was too lipophilic, resulting in high activity concentrations in the hepatobiliary system regardless of the biomolecular targeting vector. To circumvent this problem, Babich and coworkers modified the ligand to include more polar heterocycles [59]. Through the addition of a carboxylic acid-containing donor or an acetate-functionalized imidazole, the off-target binding of these bioconjugates was decreased dramatically. More specifically, these ^{99m}Tc-bearing compounds are typically eliminated through the kidneys and have low uptake in the hepatobiliary system. This study reinforces the notion that simple modifications to the structure of the chelator can have a dramatic influence on the distribution and effectiveness of ^{99m}Tc-labeled bioconjugates.

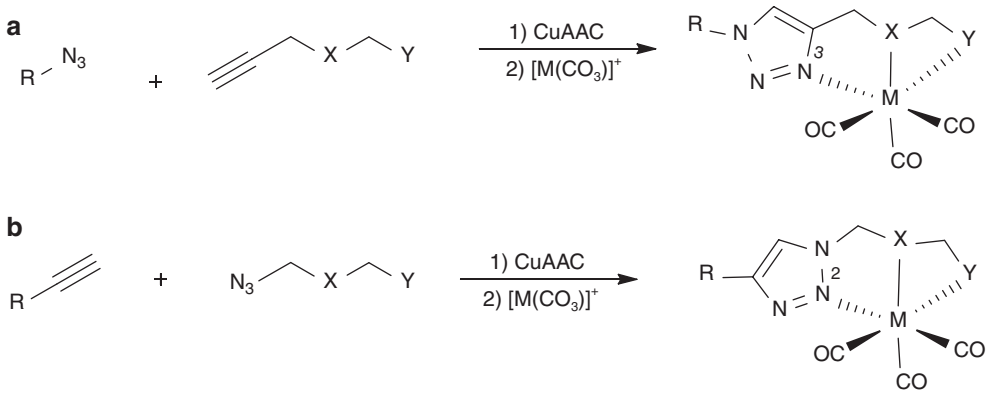

Fig. 12 Examples of the "click-to-chelate" concept [6]. (**a**) A "regular" click ligand and (**b**) an "inverse" click ligand. X and Y represent various donor atoms (*e.g.* O, N, S)

Next-Generation ^{99m}Tc Radiopharmaceuticals

^{99m}Tc-Labeled Radiopharmaceuticals that Target Prostate-Specific Membrane Antigen (PSMA)

Improvements in chelator design have led to the advent of a new generation of ^{99m}Tc-based radiopharmaceuticals. One recent example of this phenomenon is the emergence of a ^{99m}Tc radiopharmaceutical for imaging PSMA, a transmembrane protein that is overexpressed on prostate cancers [73]. By linking a suitable chelator for ^{99m}Tc(I) to a PSMA inhibitor, Babich and coworkers were able to produce an imaging agent with high tumor uptake and good clearance from nontarget tissue [81]. The product—which is called [^{99m}Tc]Tc-trofolastat and can be produced in an instant kit—has successfully completed a phase II clinical trial focused on the detection of intermediate- and high-grade prostate cancers prior to radical prostatectomy [95].

The development of [^{99m}Tc]Tc-trofolastat provides an excellent case study in the creation of a "next-generation" ^{99m}Tc-labeled radiopharmaceutical. Early in the development of [^{99m}Tc]Tc-trofolastat, two compounds composed of glutamate-urea inhibitors of PSMA, referred to in the literature as MIP-1404 and MIP-1405 (Fig. 13a, b), were prepared and used to visualize tumors in the prostate bed and metastatic disease in the bone and lymph nodes [73]. The chelators used in these imaging agents are both based on two imidazole derivatives and contain three nitrogen atoms bound to ^{99m}Tc(I); they differ in the pharmacokinetic modifying groups attached to the chelate. Each imidazole in MIP-1405 has one terminal carboxymethyl group, whereas MIP-1404 has a biscarboxymethyl amino-2-oxoethyl group attached to each heterocycle. In a comparative clinical trial, MIP-1404 showed low uptake in the kidney and demonstrated more lesions than MIP-1405, which produced higher activity concentrations in the kidneys [96]. MIP-1404—which would later become [^{99m}Tc]Tc-trofolastat—was ultimately selected as the lead compound for further testing. In a clinical trial, it identified 94% of prostate cancer lesions, higher than the 86% detected through MRI. The sensitivity and specificity of [^{99m}Tc]Tc-trofolastat toward positive lymph nodes were 33.3% and 88.4%, respectively, and the sensitivity increased to 50.0% when patients receiving androgen deprivation therapy were excluded. Interestingly, MRI results in patients under androgen deprivation therapy had much lower sensitivity (15.8%) but somewhat higher specificity (96.2%). For the sake of clarity, in the context of imaging studies, sensitivity refers to the proportion of true positive results, while specificity refers to the proportion of true negative results [97].

Another recently reported PSMA-targeted imaging agent is [^{99m}Tc]Tc-PSMA I&S [98]. This radiopharmaceutical is based on a molecule that had previously been radiolabeled with indium-111 using a DOTA chelator. However, due to the high cost and limited availability of ^{111}In, the development of technetium analogue was pursued. Synthetic modifications were performed to remove the DOTA chelator and replace it with a N_3S mercaptoacetyl triserine ligand which forms stable ^{99m}Tc(V) complex (Fig. 13c). Although prior *in vitro* studies determined that the IC_{50} for the ^{99m}Tc derivative was fivefold higher than that of the ^{111}In version, biodistribution studies showed that the two constructs produced similar activity concentrations in PSMA-positive LNCaP tumors at 1 h postinjection: 8.1 ± 1.1 and 8.3 ± 3.3% ID/g for the ^{111}In- and ^{99m}Tc-labeled compounds, respectively. While clinical results with a limited number of patients are promising, they must necessarily be regarded as preliminary.

^{99m}Tc-Labeled Agents for the Imaging of Neuroendocrine Tumors

Neuroendocrine tumors (NETs) typically overexpress somatostatin receptors. As a result, a number of different radiopharmaceuticals have been developed for imaging this target, including ^{111}In-DPTA-octreotide (Octreoscan™) and several ^{68}Ga-labeled peptides (including DOTA-TOC, DOTA-TATE, and DOTA-NOC) [99–102]. While [^{68}Ga]Ga-DOTA-TATE (NETSPOT™) has received approval for imaging NETs, it is nonetheless costly and requires access to a ^{68}Ge/^{68}Ga generator. To address this problem, work has been ongoing on the development of a ^{99m}Tc-labeled somatostatin-targeting imaging agent, with one example [^{99m}Tc]Tc-HYNIC-TOC (Fig. 13d) [103]. While this tracer showed greater sensitivity than [^{111}In]In-DTPA-octreotide, it also suffers from significant nontarget uptake in the pancreas. Consequently, there is an opportunity to develop more effective ^{99m}Tc-labeled radiopharmaceuticals for imaging NETs.

^{99m}Tc-Labeled Agents that Target Angiogenesis

Recently, a tracer known as [^{99m}Tc]Tc-3PRGD$_2$ was developed for imaging diseases characterized by increased angiogenesis. This agent—which is currently in phase I trials [104–106]—targets the $\alpha_v\beta_3$ integrin that is overexpressed on the endothelial cells of newly formed blood vessels. Targeting is achieved through the use of the well-known cyclic RGD dimer peptide, and a PEG-4-modified variant HYNIC is used for radiolabeling with ^{99m}Tc (Fig. 13e) [107]. [^{99m}Tc]Tc-3PRGD$_2$ is currently the subject of three clinical trials for patients with rheumatoid arthritis (RA), esophageal cancer, or breast cancers [108]. In preclinical studies, [^{99m}Tc]Tc-3PRGD$_2$ was able to detect arthritic joints as early as 30 min post-injection, and the lesions were still visible at 6 h post-injection [105]. The tracer produced high uptake in the kidneys and yielded a positive correlation between the severity of the arthritic disease and the uptake values in the joints, with more severe cases displaying higher activity concentrations.

Because they are capable of imaging a target that is associated with different disease states, radiopharmaceuticals

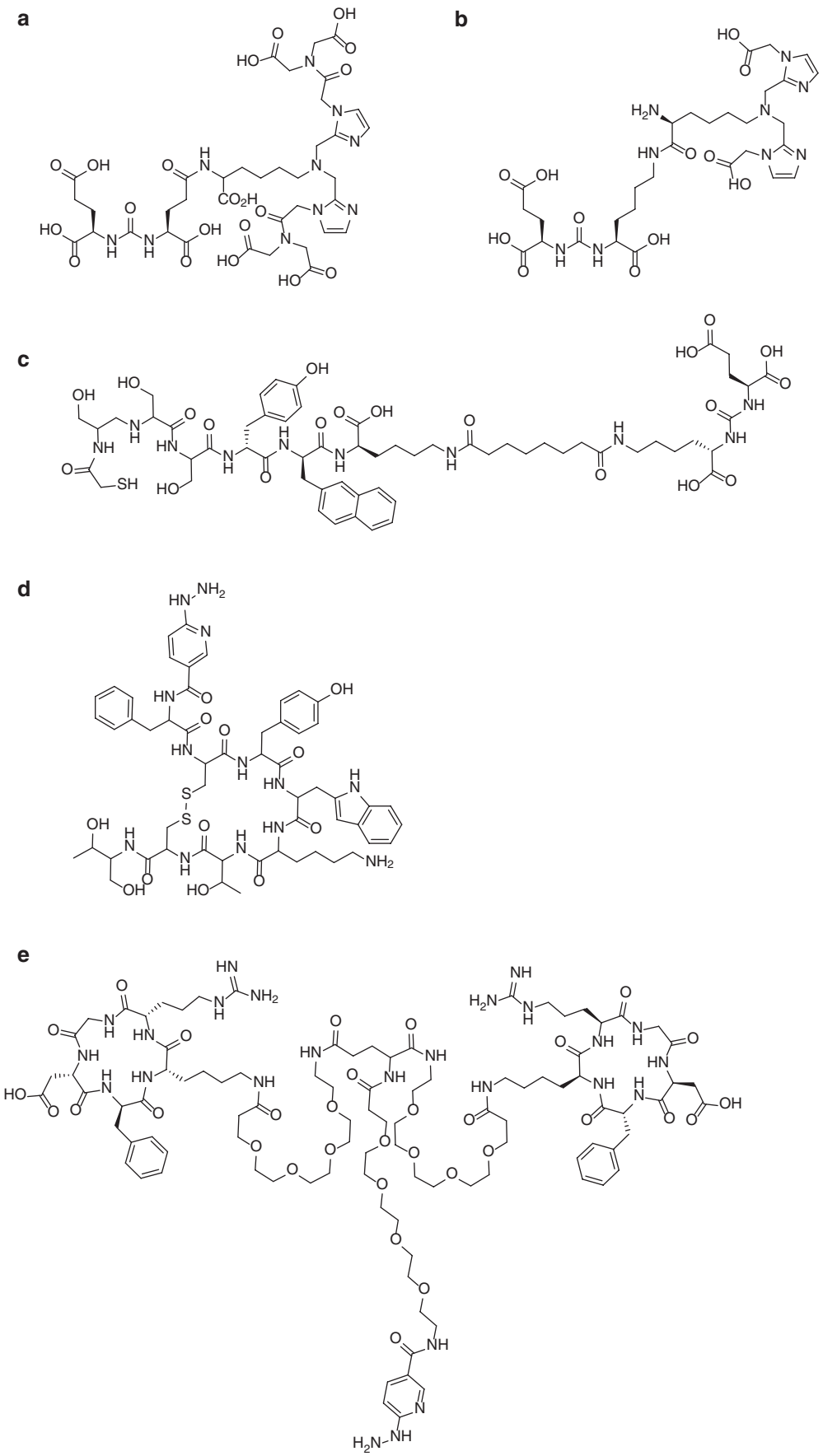

Fig. 13 Technetium-binding radiopharmaceuticals that are currently in clinical trials. (**a**) MIP-1404; (**b**) MIP-1405 [73]; (**c**) PSMA I&S [98]; (**d**) HYNIC-TOC [103]; and (**e**) $3PRGD_2$ [110]

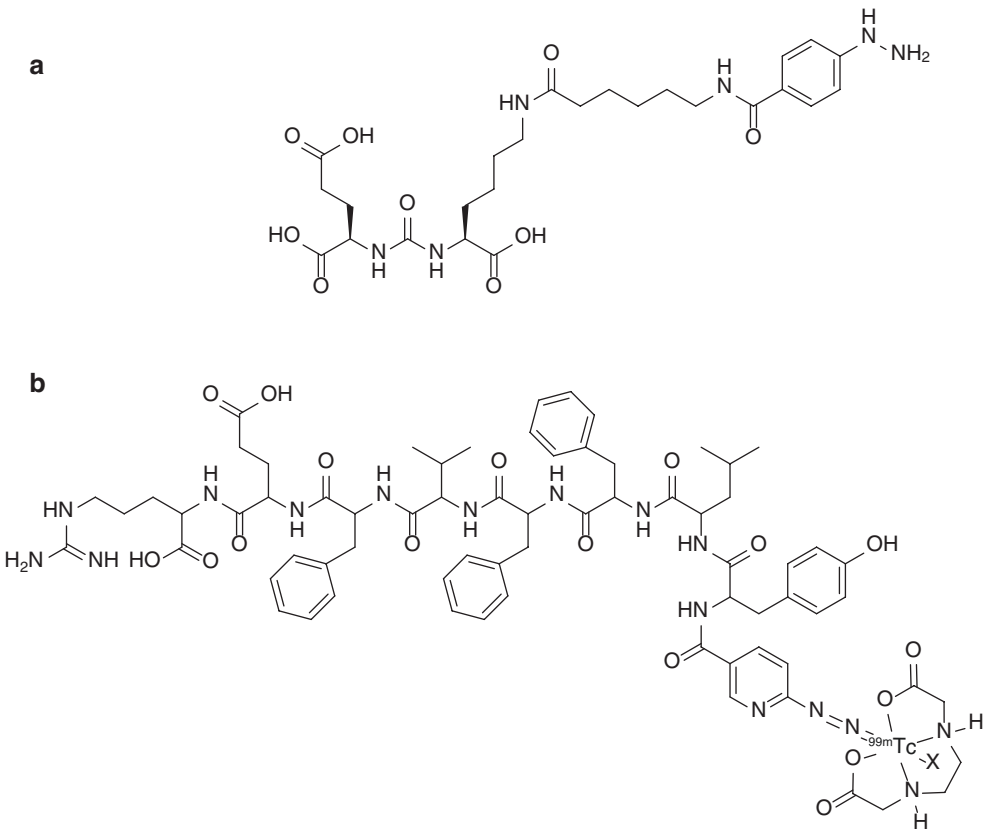

Fig. 14 Two recent examples of targeted ^{99m}Tc-labeled radiopharmaceuticals: (**a**) HYNIC-ALUG [108] and (**b**) [^{99m}Tc]Tc-HYNIC-H6F (X is likely H_2O or Cl^-) [109]

like [^{99m}Tc]Tc-3PRGD$_2$ have the potential to have widespread clinical utility. A comparative study of [^{99m}Tc]Tc-3PRGD$_2$ and [^{99m}Tc]Tc-MIBI showed comparable uptake for the two tracers in breast cancer lesions [106]. [^{99m}Tc]Tc-3PRGD$_2$ was capable of distinguishing between benign lesions and breast cancer as well as detecting ductal carcinoma *in situ*. [^{99m}Tc]Tc-3PRGD$_2$ had sensitivity, specificity, and accuracy values of 89.3%, 90.9%, and 89.7%, respectively, compared to 87.5%, 72.7%, and 82.1%, respectively, for [^{99m}Tc]Tc-MIBI. There continues to be a major unmet clinical need for radiopharmaceuticals that can help characterize suspicious lesions that are seen by mammography and reduce the number of unnecessary biopsies.

^{99m}Tc-Labeled Agents with Interesting Preclinical Data

A recent publication described [^{99m}Tc]Tc-HYNIC-ALUG, an agent for imaging prostate cancer that combines the HYNIC core with a small molecule glutamate-urea-lysine PSMA inhibitor (Fig. 14a) [109]. The radiolabeling reaction was performed in 15 min at 100 °C, resulting in a radiochemical purity of >99% and specific activity of 200 GBq/μmol. In a biodistribution study, the compound produced very high activity concentrations in LNCaP tumors at early time points (14 and 19%ID/g at 1 and 2 h, respectively) as well as low non-specific binding. Due to its rapid rate of excretion, the effective dose delivered by the agent was 8.4×10^{-4} mSv/MBq, which is lower than that created by MIP-1404 and MIP-1405 (8.78×10^{-3} and 7.87×10^{-3} mSv/MBq, respectively).

Another recent publication combined a HER2-targeted peptide with a HYNIC ligand for the imaging of breast cancer (Fig. 14b) [110]. In this case, the radiolabeling reaction was performed in 25 min, producing the tracer in a radiochemical purity greater than 95% and a specific activity of 35 MBq/nmol. A biodistribution study in mice bearing MDA-MB-453 xenografts produced tumor activity concentrations of 2.5 ± 0.1, 0.7 ± 0.2, and 0.2 ± 0.1 %ID/g at 0.5, 1, and 2 h, respectively. Importantly, these values were significantly higher at most time points than those in nontarget tissues such as the heart, spleen, intestine, and muscle. Due to its rapid accumulation in tumor tissue and low background uptake, [^{99m}Tc]Tc-HYNIC-H6F has the potential to be used to monitor HER2 expression non-invasively. This could help improve the detection and characterization of breast cancer as well as inform choices of therapy. However, further preclinical development is needed to increase the uptake and retention of the agent in tumor tissue, an improvement that could be driven by the modification of the tracer's ligands.

The Bottom Line

A key message that we hope to convey with this chapter is that while ^{99m}Tc remains a mainstay of nuclear medicine, the development of next-generation ^{99m}Tc radiopharmaceuticals

has not kept pace with the advancement of the field as a whole. That said, the impressive results recently seen with several PSMA-targeted constructs illustrate that advancements in ^{99m}Tc chemistry can create transformative diagnostic tools that can improve patient management. The field must build on this recent momentum and continue to exploit the low cost and low dose burden of ^{99m}Tc as well as the logistical advantages offered by instant kits. The latter are vastly simpler than the multi-step and automated production methods typically used with a large number of other radionuclides and thus help to lower the cost and time required to translate novel imaging agents.

With respect to opportunities, the ability to image infection and inflammation remains an important unmet medical need. Despite early, unsuccessful attempts to use ^{99m}Tc-labeled antibiotics and peptides, new ^{99m}Tc-based agents that bind biomarkers unique to these conditions would offer a cost-effective way to diagnose a wide range of diseases and to monitor response to therapy. The same is true in the field of immuno-oncology. Here, major investments are being made in pharmaceuticals that stimulate the immune system to attack tumors. Responses, particularly in melanoma, have been dramatic. However, there is a serious unmet medical need for techniques for monitoring early response to these expensive treatments, many of which can come with serious side effects. As multiple imaging sessions for assessing immune cell migration and tumor response are needed, ^{99m}Tc is the ideal medical radionuclide for such an imaging agent.

References

1. Perrier C, Segrè E. Radioactive isotopes of element 43. Nature. 1937;140:193–4.
2. Abram U, Alberto R. Technetium and rhenium – Coordination chemistry and nuclear medical applications. J Braz Chem Soc. 2006;17(8):1486–500.
3. Méndez-Rojas MA, Kharisov BI, Tsivadze AY. Recent advances on technetium complexes: coordination chemistry and medical applications. J Coord Chem. 2006;59(1):1–63.
4. Morais GR, Paulo A, Santos I. Organometallic complexes for SPECT imaging and/or radionuclide therapy. Organometallics. 2012;31(16):5693–714.
5. Amato I. Nuclear medicine's conundrum. Chem Eng News. 2009;87(36):58–64.
6. Kluba CA, Mindt TL. Click-to-Chelate: development of technetium and rhenium-tricarbonyl labeled radiopharmaceuticals. Molecules. 2013;18(3):3206–26.
7. Pillai MR, Dash A, Knapp FF Jr. Sustained availability of ^{99m}Tc: possible paths forward. J Nucl Med. 2013;54(2):313–23.
8. Boschi A, Martini P, Pasquali M, Uccelli L. Recent achievements in Tc-99m radiopharmaceutical direct production by medical cyclotrons. Drug Dev Ind Pharm. 2017;43(9):1402–12.
9. Ross CA, Diamond WT. Predictions regarding the supply of ^{99}Mo and ^{99m}Tc when NRU ceases production in 2018. Phys Can. 2015;71(3):131–8.
10. Jang J, Yamamoto M, Uesaka M. Design of an X-band electron linear accelerator dedicated to decentralized ^{99}Mo/^{99m}Tc supply: From beam energy selection to yield estimation. Phys Rev Accel Beams. 2017;20(10):104701.
11. Schaffer P, Bénard F, Bernstein A, Buckley K, Celler A, Cockburn N, et al. Direct production of ^{99m}Tc via ^{100}Mo(p,2n) on small medical cyclotrons. Phys Procedia. 2015;66:383–95.
12. Lebowitz E, Richards P. Radionuclide generator systems. Semin Nucl Med. 1974;4(3):257–68.
13. Jones AG, Davison A. The chemistry of technetium I, II, III and IV. Int J Appl Radiat Isot. 1982;33(10):867–74.
14. Papagiannopoulou D. Technetium-99m radiochemistry for pharmaceutical applications. J Label Compd Radiopharm. 2017;60(11):502–20.
15. Technetium-99m Radiopharmaceuticals: Manufacture of Kits. International Atomic Energy Agency, 2008. Technical Reports Report No.: 466.
16. Wong E, Fauconnier T, Bennett S, Valliant J, Nguyen T, Lau F, et al. Rhenium(V) and technetium(V) oxo complexes of an N2N'S peptidic chelator: evidence of interconversion between the syn and anti conformations. Inorg Chem. 1997;36(25):5799–808.
17. Alberto R, Schibli R, Egli A, Schubiger AP, Abram U, Kaden TA. A Novel organometallic aqua complex of technetium for the labeling of biomolecules: synthesis of $[^{99m}Tc(OH_2)_3(CO)_3]^+$ from $[^{99m}TcO_4]^-$ in aqueous solution and its reaction with a bifunctional ligand. J Am Chem Soc. 1998;120(31):7987–8.
18. Alberto R, Schibli R, Egli A, Schubiger PA, Herrmann WA, Artus G, et al. Metal-carbonyl syntheses XXII. Low-pressure carbonylation of $[MOCl_4)]^-$ and $[Mo_4]^-$: the technetium(I) and rhenium(I) complexes $[NEt_4]_2[MCl_3(CO_3]$. J Organomet Chem. 1995;493(1–2):119.
19. Egli A, Alberto R, Tannahill L, Schibli R, Abram U, Schaffland A, et al. Organometallic ^{99m}Tc-aquaion labels peptide to an unprecedented high specific activity. J Nucl Med. 1999;40(11):1913–7.
20. Schibli R, Schwarzbach R, Alberto R, Ortner K, Schmalle H, Dumas C, et al. Steps toward high specific activity labeling of biomolecules for therapeutic application: preparation of precursor $[^{188}Re(H_2O)_3(CO)_3]^+$ and synthesis of tailor-made bifunctional ligand systems. Bioconjug Chem. 2002;13(4):750–6.
21. Deutsch E, Libson K, Vanderheyden JL, Ketring AR, Maxon HR. The chemistry of rhenium and technetium as related to the use of isotopes of these elements in therapeutic and diagnostic nuclear medicine. Int J Rad Appl Instrum B. 1986;13(4):465–77.
22. Farwell MD, Pryma DA, Mankoff DA. PET/CT imaging in cancer: current applications and future directions. Cancer. 2014;120(22):3433–45.
23. Zolle I, editor. Technetium-99m pharmaceuticals: preparation and quality control in nuclear medicine. Berlin/Heidelberg: Springer; 2007.
24. Coover LR. The role of technetium tc 99m sestamibi in the early detection of breast carcinoma. Hosp Physician. 1999;35(2):16–21.
25. Berman DS, Kiat H, Friedman JD, Wang FP, Van Train K, Matzer L, et al. Separate acquisition rest thallium-201/stress technetium-99m sestamibi dual-isotope myocardial perfusion single-photon emission computed tomography: a clinical validation study. J Am Coll Cardiol. 1993;22(5):1455–64.
26. Wackers FJ, Berman DS, Maddahi J, Watson DD, Beller GA, Strauss HW, et al. Technetium-99m hexakis 2-methoxyisobutyl isonitrile: human biodistribution, dosimetry, safety, and preliminary comparison to thallium-201 for myocardial perfusion imaging. J Nucl Med. 1989;30(3):301–11.
27. Yaes RJ. Clinical review, Tc 99m Sestamibi. U.S. Food and Drug Administration 2 Apr 2008. NDA 19-785. https://www.fda.gov/downloads/Drugs/.../DevelopmentResources/ucm072825.pdf. Accessed 7 Apr 2018.
28. Kelly JD, Forster AM, Higley B, Archer CM, Booker FS, Canning LR, et al. Technetium-99m-tetrofosmin as a new

radiopharmaceutical for myocardial perfusion imaging. J Nucl Med. 1993;34(2):222–7.
29. Sinusas AJ, Shi Q, Saltzberg MT, Vitols P, Jain D, Wackers FJ, et al. Technetium-99m-tetrofosmin to assess myocardial blood flow: experimental validation in an intact canine model of ischemia. J Nucl Med. 1994;35(4):664–71.
30. Myoview 30 mL Kit for the preparation of technetium Tc99m tetrofosmin for Injection. GE Healthcare. 2011. http://www3.gehealthcare.com/en/products/categories/nuclear_imaging_agents/nuclear_pharmacies. Accessed Oct 2017.
31. Yazdani A, Bilton H, Vito A, Genady AR, Rathmann SM, Ahmad Z, et al. A bone-seeking trans-cyclooctene for pretargeting and bioorthogonal chemistry: a proof of concept study using ^{99m}Tc- and ^{177}Lu-labeled tetrazines. J Med Chem. 2016;59(20):9381–9.
32. Jurisson S, Berning D, Jia W, Ma DS. Coordination-compounds in nuclear-medicine. Chem Rev. 1993;93(3):1137–56.
33. Libson K, Deutsch E, Barnett BL. Structural characterization of a technetium-99-diphosphonate complex. Implications for the chemistry of technetium-99m skeletal imaging agents. J Am Chem Soc. 1980;102(7):2476–8.
34. Atkins HL. Radiopharmaceuticals. Phys Rep. 1975;21(6):315–67.
35. Junankar S, Shay G, Jurczyluk J, Ali N, Down J, Pocock N, et al. Real-time intravital imaging establishes tumor-associated macrophages as the extraskeletal target of bisphosphonate action in cancer. Cancer Discov. 2015;5(1):35–42.
36. DMSA kit for the preparation of technetium Tc99m Succimer Injection. GE Healthcare. 2006. http://www3.gehealthcare.com/en/products/categories/nuclear_imaging_agents/nuclear_pharmacies. Accessed Oct 2017.
37. Handmaker H, Young BW, Lowenstein JM. Clinical experience with ^{99m}Tc-DMSA (dimercaptosuccinic acid), a new renal-imaging agent. J Nucl Med. 1975;16(1):28–32.
38. de Lange MJ, Piers DA, Kosterink JG, van Luijk WH, Meijer S, de Zeeuw D, et al. Renal handling of technetium-99m DMSA: evidence for glomerular filtration and peritubular uptake. J Nucl Med. 1989;30(7):1219–23.
39. Draximage DTPA kit for the preparation of technetium Tc99m pentate injection. GE Healthcare. 2016. http://www.draximage.com/products/us/draximage-dtpa/. Accessed Oct 2017.
40. Kabasakal L. Technetium-99m ethylene dicysteine: a new renal tubular function agent. Eur J Nucl Med. 2000;27(3):351–7.
41. Technescan MAG3 kit for the preparation of technetium Tc99m mertiatide. Curium Pharma. 2015. https://curiumpharma.com/wp-content/uploads/2017/02/Tscan-MAG3-a096i0-in-1015.pdf. Accessed Oct 2017.
42. Klingensmith WC 3rd, Briggs DE, Smith WI. Technetium-99m-MAG3 renal studies: normal range and reproducibility of physiologic parameters as a function of age and sex. J Nucl Med. 1994;35(10):1612–7.
43. Eshima D, Fritzberg AR, Taylor A Jr. ^{99m}Tc renal tubular function agents: current status. Semin Nucl Med. 1990;20(1):28–40.
44. Jurgens S, Herrmann WA, Kuhn FE. Rhenium and technetium based radiopharmaceuticals: development and recent advances. J Organomet Chem. 2014;751:83–9.
45. Ponto JA. Mechanisms of radiopharmaceutical localization (Norenberg J, editor). Albuquerque: University of New Mexico College of Pharmacy 2012;16(4). Program No. 0039-000-12-164-H04-P 2.5.
46. Ceretec kit for the preparation of technetium Tc99m exametazime injection. GE Healthcare. 2013. http://www3.gehealthcare.com/en/products/categories/nuclear_imaging_agents/nuclear_pharmacies. Accessed Oct 2017.
47. Neirinckx RD, Canning LR, Piper IM, Nowotnik DP, Pickett RD, Holmes RA, et al. Technetium-99m d,l-HM-PAO: a new radiopharmaceutical for SPECT imaging of regional cerebral blood perfusion. J Nucl Med. 1987;28(2):191–202.
48. Robins PD, Salazar I, Forstrom LA, Mullan BP, Hung JC. Biodistribution and radiation dosimetry of stabilized ^{99m}Tc-exametazine-labeled leukocytes in normal subjects. J Nucl Med. 2000;41(5):934–40.
49. Chervu LR, Nunn AD, Loberg MD. Radiopharmaceuticals for hepatobiliary imaging. Semin Nucl Med. 1982;12(1):5–17.
50. Krishnamurthy GT, Turner FE. Pharmacokinetics and clinical application of technetium 99m-labeled hepatobiliary agents. Semin Nucl Med. 1990;20(2):130–49.
51. Weissmann HS, Frank MS, Bernstein LH, Freeman LM. Rapid and accurate diagnosis of acute cholecystitis with 99mTc-HIDA cholescintigraphy. AJR Am J Roentgenol. 1979;132(4):523–8.
52. Neurolite kit for the preparation of technetium Tc99m bicisate for injection. Lantheus Medical Imaging. 2015. http://www.lantheus.com/assets/Neurolite-US-PI-513073-0415-format-6-1-29-2016.pdf. Accessed Oct 2017.
53. Vanbilloen HP, Cleynhens BJ, Verbruggen AM. Importance of the two ester functions for the brain retention of ^{99m}Tc-labelled ethylene dicysteine diethyl ester (^{99m}Tc-ECD). Nucl Med Biol. 1998;25(6):569–75.
54. Vallabhajosula S, Zimmerman RE, Picard M, Stritzke P, Mena I, Hellman RS, et al. Technetium-99m ECD: a new brain imaging agent: in vivo kinetics and biodistribution studies in normal human subjects. J Nucl Med. 1989;30(5):599–604.
55. Kit for the preparation of technetium Tc 99m sulfur colloid injection. Rev. 1.1 Pharmalucence. 2013. http://www.pharmalucence.com/images/SC_PI.pdf. Accessed Oct 2017.
56. Michenfelder MM, Bartlett LJ, Mahoney DW, Herold TJ, Hung JC. Particle-size and radiochemical purity evaluations of filtered ^{99m}Tc-sulfur colloid prepared with different heating times. J Nucl Med Technol. 2014;42(4):283–8.
57. Kern KA, Rosenberg RJ. Preoperative lymphoscintigraphy during lymphatic mapping for breast cancer: improved sentinel node imaging using subareolar injection of technetium 99m sulfur colloid. J Am Coll Surg. 2000;191(5):479–89.
58. Dewanjee MK. The chemistry of ^{99m}Tc-labeled radiopharmaceuticals. Semin Nucl Med. 1990;20(1):5–27.
59. Maresca KP, Marquis JC, Hillier SM, Lu G, Femia FJ, Zimmerman CN, et al. Novel polar single amino acid chelates for technetium-99m tricarbonyl-based radiopharmaceuticals with enhanced renal clearance: application to octreotide. Bioconjug Chem. 2010;21(6):1032–42.
60. Meszaros LK, Dose A, Biagini SCG, Blower PJ. Hydrazinonicotinic acid (HYNIC) – Coordination chemistry and applications in radiopharmaceutical chemistry. Inorg Chim Acta. 2010;363(6):1059–69.
61. Ogawa K, Mukai T, Inoue Y, Ono M, Saji H. Development of a novel ^{99m}Tc-chelate-conjugated bisphosphonate with high affinity for bone as a bone scintigraphic agent. J Nucl Med. 2006;47(12):2042–7.
62. Zhang XY, Yu PR, Yang YP, Hou YQ, Peng C, Liang ZG, et al. ^{99m}Tc-labeled 2-arylbenzothiazoles: a beta imaging probes with favorable brain pharmacokinetics for single-photon emission computed tomography. Bioconjug Chem. 2016;27(10):2493–504.
63. Eckelman W, Richards P. Instant ^{99m}Tc-DTPA. J Nucl Med. 1970;11(12):761.
64. Abrams MJ, Juweid M, tenKate CI, Schwartz DA, Hauser MM, Gaul FE, et al. Technetium-99m-human polyclonal IgG radiolabeled via the hydrazino nicotinamide derivative for imaging focal sites of infection in rats. J Nucl Med. 1990;31(12):2022–8.
65. Garcia MF, Zhang X, Shah M, Newton-Northup J, Cabral P, Cerecetto H, et al. ^{99m}Tc-bioorthogonal click chemistry reagent for in vivo pretargeted imaging. Bioorg Med Chem. 2016;24(6):1209–15.
66. von Guggenberg E, Behe M, Behr TM, Saurer M, Seppi T, Decristoforo C. ^{99m}Tc-labeling and in vitro and in vivo evaluation

of HYNIC- and (Na-His)acetic acid-modified [D-Glu^1]-minigastrin. Bioconjug Chem. 2004;15(4):864–71.
67. Babich JW, Solomon H, Pike MC, Kroon D, Graham W, Abrams MJ, et al. Technetium-99m-labeled hydrazino nicotinamide derivatized chemotactic peptide analogs for imaging focal sites of bacterial infection. J Nucl Med. 1993;34(11):1964–74.
68. Faintuch BL, Santos RLSR, Souza ALFM, Hoffman TJ, Greeley M, Smith CJ. ^{99m}Tc-HYNIC-Bombesin (7–14)NH_2: Radiochemical evaluation with co-ligands EDDA (EDDA = ethylenediamine-N,N ′-diacetic acid), tricine, and nicotinic acid. Synth React Inorg Met Org Chem. 2005;35(1):43–51.
69. Vito A, Alarabi H, Czorny S, Beiraghi O, Kent J, Janzen N, et al. A ^{99m}Tc-labelled tetrazine for bioorthogonal chemistry. synthesis and biodistribution studies with small molecule *trans*-cyclooctene derivatives. PLoS One. 2016;11(12):e0167425.
70. von Guggenberg E, Sarg B, Lindner H, Alafort LM, Mather SJ, Moncayo R, et al. Preparation via coligand exchange and characterization of [^{99m}Tc-EDDA-HYNIC-D-Phe$_1$,Tyr$_3$]octreotide (^{99m}Tc-EDDA/HYNIC-TOC). J Label Compd Radiopharm. 2003;46(4):307–18.
71. Alberto R, Schibli R, Schubiger AP, Abram U, Pietzsch HJ, Johannsen B. First application of *fac*-[^{99m}Tc$(OH_2)_3(CO)_3]^+$ in bioorganometallic chemistry: design, structure, and in vitro affinity of a 5-HT_{1A} receptor ligand labeled with ^{99m}Tc. J Am Chem Soc. 1999;121(25):6076–7.
72. Bilton HA, Ahmad Z, Janzen N, Czorny S, Valliant JF. Preparation and evaluation of ^{99m}Tc-labeled tridentate chelates for pre-targeting using bioorthogonal chemistry. J Vis Exp. 2017;120:e55188.
73. Goffin KE, Joniau S, Tenke P, Slawin K, Klein EA, Stambler N, et al. Phase 2 study of ^{99m}Tc-trofolastat SPECT/CT to identify and localize prostate cancer in intermediate- and high-risk patients undergoing radical prostatectomy and extended pelvic LN dissection. J Nucl Med. 2017;58(9):1408–13.
74. Banerjee SR, Levadala MK, Lazarova N, Wei L, Valliant JF, Stephenson KA, et al. Bifunctional single amino acid chelates for labeling of biomolecules with the {$Tc(CO)_3$}+ and {$Re(CO)_3$}+ Cores. Crystal and molecular structures of [ReBr$(CO)_3(H_2NCH_2C_5H_4N)$], [$ReCO)_3${$(C_5H_4NCH_2)_2NH$}]Br, [$Re(CO)_3${$(C_5H_4NCH_2)_2NCH_2CO_2H$}]Br, [$Re(CO)_3${X(Y)$NCH_2CO_2CH_2CH_3$}]Br (X =Y = 2-pyridylmethyl; X = 2-pyridylmethyl, Y = 2-(1-methylimidazolyl)methyl; X = Y) 2-(1-methylimidazolyl)methyl), [$ReBr(CO)_3${$(C_5H_4NCH_2)NH(CH_2C_4H_3S)$}], and [$Re(CO)_3${$(C_5H_4NCH_2)N(CH_2C_4H_3S)(CH_2CO_2)$}]. Inorg Chem. 2002;41(24):6417–6425.
75. Bayly SR, Fisher CL, Storr T, Adam MJ, Orvig C. Carbohydrate conjugates for molecular imaging and radiotherapy: Tc-99m(I) and Re-186(I) tricarbonyl complexes of N-(2′-hydroxybenzyl)-2-amino-2-deoxy-D-glucose. Bioconjug Chem. 2004;15(4):923–6.
76. Karagiorgou O, Patsis G, Pelecanou M, Raptopoulou CP, Terzis A, Siatra-Papastaikoudi T, et al. (S)-(2-(2′-Pyridyl)ethyl)cysteamine and (S)-(2-(2′-pyridyl)ethyl)-d,l-homocysteine as ligands for the "*fac*-[$M(CO)_3]^+$" (M = Re, ^{99m}Tc) core. Inorg Chem. 2005;44(12):4118–20.
77. Lazarova N, Babich J, Valliant J, Schaffer P, James S, Zubieta J. Thiol- and thioether-based bifunctional chelates for the $[M(CO)_3]^+$ core (M = Tc, Re). Inorg Chem. 2005;44(19):6763–70.
78. Liu Y, Pak JK, Schmutz P, Bauwens M, Mertens J, Knight H, et al. Amino acids labeled with [^{99m}Tc$(CO)_3]^+$ and recognized by the L-type amino acid transporter LAT1. J Am Chem Soc. 2006;128(50):15996–7.
79. Schweinsberg C, Maes V, Brans L, Blauenstein P, Tourwe DA, Schubiger PA, et al. Novel glycated [^{99m}Tc$(CO)_3$]-labeled bombesin analogues for improved targeting of gastrin-releasing peptide receptor-positive tumors. Bioconjug Chem. 2008;19(12):2432–9.
80. Banerjee SR, Pullambhatla M, Foss CA, Falk A, Byun Y, Nimmagadda S, et al. Effect of chelators on the pharmacokinetics of Tc-99m-labeled imaging agents for the prostate-specific membrane antigen (PSMA). J Med Chem. 2013;56(15):6108–21.
81. Hillier SM, Maresca KP, Lu G, Merkin RD, Marquis JC, Zimmerman CN, et al. ^{99m}Tc-labeled small-molecule inhibitors of prostate-specific membrane antigen for molecular imaging of prostate cancer. J Nucl Med. 2013;54(8):1369–76.
82. Jiang H, Kasten BB, Liu H, Qi S, Liu Y, Tian M, et al. Novel, cysteine-modified chelation strategy for the incorporation of $[M^I(CO)_3]^+$(M = Re, ^{99m}Tc) in an α-MSH peptide. Bioconjug Chem. 2012;23(11):2300–12.
83. Alberto R, Ortner K, Wheatley N, Schibli R, Schubiger AP. Synthesis and properties of boranocarbonate: a convenient in situ co source for the aqueous preparation of [^{99m}Tc$(OH_2)_3(CO)_3]^+$. J Am Chem Soc. 2001;123(13):3135–6.
84. Wilson AA, Jin L, Garcia A, DaSilva JN, Houle S. An admonition when measuring the lipophilicity of radiotracers using counting techniques. Appl Radiat Isot. 2001;54(2):203–8.
85. Stein WH, Moore S. The free amino acids of human blood plasma. J Biol Chem. 1954;211(2):915–26.
86. Schibli R, La Bella R, Alberto R, Garcia-Garayoa E, Ortner K, Abram U, et al. Influence of the denticity of ligand systems on the in vitro and in vivo behavior of ^{99m}tc(i)-tricarbonyl complexes: a hint for the future functionalization of biomolecules. Bioconjug Chem. 2000;11(3):345–51.
87. Eckelman WC, Kilbourn MR, Joyal JL, Labiris R, Valliant JF. Justifying the number of animals for each experiment. Nucl Med Biol. 2007;34(3):229–32.
88. Jones AG, Abrams MJ, Davison A, Brodack JW, Toothaker AK, Adelstein SJ, et al. Biological studies of a new class of technetium complexes: the hexakis(alkylisonitrile)technetium(I) cations. Int J Nucl Med Biol. 1984;11(3–4):225–34.
89. Brown RP, Delp MD, Lindstedt SL, Rhomberg LR, Beliles RP. Physiological parameter values for physiologically based pharmacokinetic models. Toxicol Ind Health. 1997;13(4):407–84.
90. Psimadas D, Baldi G, Ravagli C, Bouziotis P, Xanthopoulos S, Franchini MC, et al. Preliminary evaluation of a ^{99m}Tc labeled hybrid nanoparticle bearing a cobalt ferrite core: in vivo biodistribution. J Biomed Nanotechnol. 2012;8(4):575–85.
91. Kendi AT, Moncayo VM, Nye JA, Galt JR, Halkar R, Schuster DM. Radionuclide therapies in molecular imaging and precision medicine. PET clin. 2017;12(1):93–103.
92. Banerjee SR, Foss CA, Castanares M, Mease RC, Byun Y, Fox JJ, et al. Synthesis and evaluation of technetium-99m- and rhenium-labeled inhibitors of the prostate-specific membrane antigen (PSMA). J Med Chem. 2008;51(15):4504–17.
93. Mindt TL, Struthers H, Brans L, Anguelov T, Schweinsberg C, Maes V, et al. "Click to chelate": synthesis and installation of metal chelates into biomolecules in a single step. J Am Chem Soc. 2006;128(47):15096–7.
94. Morais M, Oliveira BL, Correia JD, Oliveira MC, Jimenez MA, Santos I, et al. Influence of the bifunctional chelator on the pharmacokinetic properties of ^{99m}Tc$(CO)_3$-labeled cyclic a-melanocyte stimulating hormone analog. J Med Chem. 2013;56(5):1961–73.
95. Scherr D, Karnes J, Slawin K, Keane T, Trabulsi E, Ellis W, et al. A phase 2 study with MIP-1404 in men with high-risk PC scheduled for RP and EPLND compared to histopathology. 2012. clinicaltrials.gov/ct2/show/NCT01667536. Acceessed 8 Apr 2018.
96. Vallabhajosula S, Nikolopoulou A, Babich JW, Osborne JR, Tagawa ST, Lipai I, et al. ^{99m}Tc-labeled small-molecule inhibitors of prostate-specific membrane antigen: pharmacokinetics and biodistribution studies in healthy subjects and patients with metastatic prostate cancer. J Nucl Med. 2014;55(11):1791–8.
97. Altman DG, Bland JM. Diagnostic tests. 1: sensitivity and specificity. BMJ. 1994;308(6943):1552.
98. Robu S, Schottelius M, Eiber M, Maurer T, Gschwend J, Schwaiger M, et al. Preclinical evaluation and first patient application of

^{99m}Tc-PSMA-I&S for SPECT imaging and radioguided surgery in prostate cancer. J Nucl Med. 2017;58(2):235–42.
99. Buchmann I, Henze M, Engelbrecht S, Eisenhut M, Runz A, Schafer M, et al. Comparison of ^{68}Ga-DOTATOC PET and ^{111}In-DTPAOC (Octreoscan) SPECT in patients with neuroendocrine tumours. Eur J Nucl Med Mol Imaging. 2007;34(10):1617–26.
100. Shi W, Johnston CF, Buchanan KD, Ferguson WR, Laird JD, Crothers JG, et al. Localization of neuroendocrine tumours with [^{111}In] DTPA-octreotide scintigraphy (Octreoscan): a comparative study with CT and MR imaging. QJM. 1998;91(4):295–301.
101. Srirajaskanthan R, Kayani I, Quigley AM, Soh J, Caplin ME, Bomanji J. The role of ^{68}Ga-DOTATATE PET in patients with neuroendocrine tumors and negative or equivocal findings on ^{111}In-DTPA-octreotide scintigraphy. J Nucl Med. 2010;51(6):875–82.
102. Wild D, Bomanji JB, Benkert P, Maecke H, Ell PJ, Reubi JC, et al. Comparison of ^{68}Ga-DOTANOC and ^{68}Ga-DOTATATE PET/CT within patients with gastroenteropancreatic neuroendocrine tumors. J Nucl Med. 2013;54(3):364–72.
103. Behera A, De K, Chandra S, Chattopadhyay S, Misra M. Synthesis, radiolabelling and biodistribution of HYNIC-Tyr^3 octreotide: a somatostatin receptor positive tumour imaging agent. J Radioanal Nucl Chem. 2011;290(1):123–9.
104. Gao S, Ma Q, Wen Q, Jia B, Liu Z, Chen Z, et al. ^{99m}Tc-3P$_4$-RGD$_2$ radiotracers for SPECT/CT of esophageal tumor. Nucl Sci Tech. 2013;24(4):040302.
105. Huang C, Zheng Q, Miao W. Study of novel molecular probe ^{99m}Tc-3PRGD2 in the diagnosis of rheumatoid arthritis. Nucl Med Commun. 2015;36(12):1208–14.
106. Ma Q, Chen B, Gao S, Ji T, Wen Q, Song Y, et al. ^{99m}Tc-3P4-RGD2 scintimammography in the assessment of breast lesions: comparative study with ^{99m}Tc-MIBI. PLoS One. 2014;9(9):e108349.
107. Jia B, Liu Z, Zhu Z, Shi J, Jin X, Zhao H, et al. Blood clearance kinetics, biodistribution, and radiation dosimetry of a kit-formulated integrin $\alpha_v\beta_3$-selective radiotracer ^{99m}Tc-$_3$PRGD$_2$ in non-human primates. Mol Imaging Biol. 2011;13(4):730–6.
108. Chen B, Zhao G, Ma Q, Ji B, Ji T, Xin H, et al. 99mTc-3P-RGD2 SPECT to monitor early response to bevacizumab therapy in patients with advanced non-small cell lung cancer. Int J Clin Exp Pathol. 2015;8(12):16064–72.
109. Xu X, Zhang J, Hu S, He S, Bao X, Ma G, et al. 99mTc-labeling and evaluation of a HYNIC modified small-molecular inhibitor of prostate-specific membrane antigen. Nucl Med Biol. 2017;48:69–75.
110. Li L, Wu Y, Wang Z, Jia B, Hu Z, Dong C, et al. SPECT/CT imaging of the novel HER2-targeted peptide probe 99mTc-HYNIC-H6F in breast cancer mouse models. J Nucl Med. 2017;58(5):821–6.